

CFD MODELLING OF DRY PRESSURE DROP IN STRUCTURED PACKING

A DISSERTATION

*Submitted in partial fulfillment of the
requirements for the award of the degree*

of

MASTER OF TECHNOLOGY

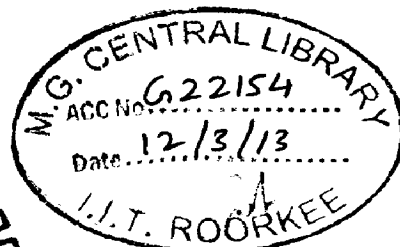
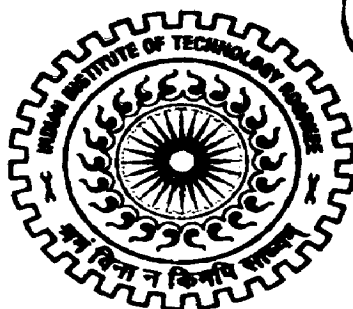
in

CHEMICAL ENGINEERING

(With Specialization in Computer Aided Process Plant Design)

By

SUNKARWAR ANUP SHRIKANT



**DEPARTMENT OF CHEMICAL ENGINEERING
INDIAN INSTITUTE OF TECHNOLOGY ROORKEE
ROORKEE -247 667 (INDIA)
JUNE, 2012**

ACKNOWLEDGEMENT

I wish to express my sincere gratitude to Dr. Gaurav and Dr. Vimal Kumar Assistant Professor, Department of Chemical Engineering, Indian Institute of Technology Roorkee, whose strengthening presence was a source of great inspiration for the successful completion of this seminar report.

I would like to take the opportunity to thanks Dr Vimal Kumar who provided whole hearted co-operation, never ending inspirations and guidance, all blending with the personal touch throughout the duration of this work. His painstaking efforts, invaluable suggestions and thorough discussions during the work have immensely contributed towards the completion of my dissertation work. This work is simply reflection of his thoughts, ideas and concepts and above his efforts.

I thank all well wishers who in any manner directly or indirectly have put a helping hand in any part of this piece of work.

SUNKARWAR ANUP SHRIKANT

Date: 15/6/2012

Place: IIT, Roorkee

Abstract

In the present work the pressure drop in Flexipac 1Y, Sulz packing and newly proposed zigzag pattern packing predicted using commercial fluid dynamic software, FLUENT 6.3, ANSYS. The geometry was pre-processed and constructed using GAMBIT software, ANSYS. The dry pressure drop in the structured packing was predicted using different turbulence models and compared with the results reported in the literature. The different viscous models used to estimate dry pressure drop are laminar, realizable k- ϵ , realizable k- ϵ with pressure gradient effect and the SST k- ω .

It is observed that the present simulated predictions using realizable k- ϵ model considering pressure gradient effects is in good agreement with the results reported in the literature. The prediction were analysed in terms of resistance factor (ψ) versus Reynolds number for the comparison of different models and literature results. A new packing is developed to give the better efficiency as compared to the Sulz EX. It has been observed that the zigzag pattern structured packing resulted into small pressure drop as compared to the Sulz EX packing. Also the wall effects of the column with the zigzag patterned geometry are reduced, which is one of the reason that the pressure drop is less as compared to the other structured packings. The flow is developed only in the inner channels for the sulz packing while it is developed in the entire computational domain of the zigzag packing leading to the less pressure drop as compared to the sulz packing. Mixing is more in the zigzag packing as compared to sulz packing due to the zigzag orientation where the flow will experience maximum directional changes. The residence time of the fluid particles will be more in the zigzag packing resulting in the good mixing. The realizable k- ϵ model considering pressure gradient effects is further extended for newly developed packing module for the future work in the CO₂ absorption process.

CONTENTS

Chapter	Title	Page No.
	Candidate's Declaration and Certificate	i
	Acknowledgement	ii
	Abstract	iii
	List of Figures	vi
	List of Tables	viii
	Nomenclature	ix
1	INTRODUCTION	1-5
	1.1 Motivation	1
	1.2 Types of packing	2
	1.2.1 Different Representative Elementary units in structured packings.	2
	1.2.2 Different types of the commercial packings	3
	1.3 Objectives	5
2	LITERATURE REVIEW	6-14
3	MODELLING AND SIMULATION	15-25
	3.1 Flexipac 1Y	16
	3.1.1 Geometry description	16
	3.1.2 Grid formation and topology	16
	3.2 Sulz EX packing	17
	3.2.1 Geometry description	17
	3.2.2 Grid topology	19
	3.3 SULZ EX packing module	20
	3.3.1 Geometry description	20
	3.3.2 Grid formation and Topology	20
	3.4 Continuity and momentum equations	21
	3.4.1 Turbulence models	21

Chapter	Title	Page no.
	3.4.1.a) k- ϵ turbulence models	21
	3.4.1 b) k- ω turbulence models	23
	3.5 Residence time analysis	24
4	CFD MODELLING OF FLEXIPAC 1Y AND SULZ EX PACKING	25-32
	4.1 Pressure drop in Flexipac 1Y structure packing	25
	4.2 Dry pressure drop in Sulz EX Packing	27
	4.3 Sulz EX packing module	33
5	CFD MODELLING OF ZIGZAG STRUCTURED PACKING	34-44
	5.1 Geometry description of Zigzag pack	34
	5.2 Grid topology	36
	5.3 Hydrodynamics and pressure drop in the Zigzag packing	37
6	CONCLUSIONS AND RECOMMENDATIONS	45
	REFERENCES	47

List of the Figures

Figure No.	Title of the Figure	Page no.
1.2.1	Different representative units from the literature. :(a) Jiangbo REU (Jiangbo et al., 2009), (b) Larachi and Petre REUs (Larachi et al., 2003; Petre et al., 2003), (c) Raynal REU (Raynal et al., 2004) and (d) Raynal periodic element (Raynal and Royon-Lebeaud,2007)	3
1.2.2	Different types of the commercial packing	4
3.1	(a) Channel direction slice for Flexipac 1Y and (b) grid topology for Flexipac 1Y	16
3.2	(a) Two sheet packing structure with 45 ⁰ inclination angle and (b) computational domain of two packing sheet included in a box.	18
3.3	(a) Computational domain and (b) grid topology of Sulz EX packing module.	20
3.5	Residence time distribution analysis	24
4.1.1	Comparison of the pressure drop in Flexipac 1Y for the different turbulence models	26
4.1.2	Comparison of pressure drop values in Flexipac 1Y predicted by different turbulence models in terms of relative errors with the results of <i>Said et al. (2011)</i> .	27
4.2.1	Comparison of the pressure drop in Sulz packing for the different turbulence models	29
4.2.3	Comparison for resistance factor between numerical simulation and the experimental data of Stockfleth and Brunner (2001).	30
4.2.4	Velocity Counters on the interior of the Sulz packing at different Reynolds number by using realizable k-ε model.	31
4.2.5	Velocity Counters on the inlet, outlet and the plane of the Sulz packing at different Reynolds number by using realizable k-ε model	32
4.3	(a) Velocity counters on the periodic and interior plane of Sulz EX packing module, and (b) pathlines inside the Sulz EX packing module	33
5.1	(a) Two sheet Zigzag packing structure with the 45 ⁰ inclination angle and (b) Computational domain of two sheets zigzag packing included in a box.	36
5.2.1	Grid topology for the zigzag packing	36

Figure No.	Title of the Figure	Page no.
5.3.1	Comparison of pressure drop of zigzag packing for different turbulence models	39
5.3.2	Comparison of pressure drop of zigzag packing for the Realizable k- ϵ turbulence models at different supercritical conditions.	40
5.3.3	Comparison of experimental and simulated values of Sulz EX packing with the simulated data for the zigzag packing.	40
5.3.4	Velocity counters on the interior of the zigzag packing at different Reynolds number by using realizable k- ϵ model	41
5.3.5	Velocity counters on the inlet and outlet planes of the zigzag packing at different Reynolds number by using realizable k- ϵ model	42
5.3.6	Pathlines inside the (a) Sulz EX packing and (b) zigzag packing.	44

List of Tables

Table no	Title of the table	Page no.
3.1	Geometrical parameters for Flexipac 1Y packing used in simulations.	16
3.2	Geometric data of Sulz EX packing (Fernandes et al., 2008).	18
3.2.1	Boundary conditions for the Sulz packing.	19
3.3.1	Boundary conditions for the Sulz packing module.	21
4.1	Pressure drop predictions in Flexipac 1Y using different turbulence models.	26
4.2.1	Pressure drop prediction in Sulz EX packing two sheet model.	28
4.2.2	Resistance factor values with different viscous models for Sulz EX packing with two sheet model.	29
5.1	Geometric parameter for Zigzag packing.	35
5.2	Boundary conditions for Zigzag packing.	37
5.3.1	Experimental conditions and physical properties of the fluids used for pressure drop in the calculations in zigzag packing.	38
5.3.2	Simulated pressure drop prediction for different turbulence models for the zigzag packing at 13.1 MPa.	38
5.3.3	Simulated pressure drop in zigzag packing under different process conditions.	39

Nomenclature

a_g	bed specific surface area, m^2/m^3
b_c	triangular channel base length, m
C_μ	constant to compute Eddy viscosity
D_c	column diameter, m
F_s	gas flow factor, m/s (kg/m^3)
h_c	triangular channel height, m
ε	dissipation rate
ω	Specific dissipation rate
k	turbulent kinetic energy, m^2s^{-2}
α_g	corrugation inclination angle, deg
ΔP	pressure drop, Pa
ε_g	packing void fraction, dimensionless
μ_t	turbulent Eddy viscosity, Pa s
ρ	density, kg/m^3
τ	Stress tensor N/m^2
G_b	turbulence kinetic energy
σ_k	turbulent Prandal number for k
σ_ε	turbulent Prandal number for ε
S_{ij}	mean strain rate tensor
Ω_{ij}	mean rate of rotation tensor

CHAPTER 1

INTRODUCTION

1.1 Motivation

Packed columns are used in many chemical processes involving absorption, CO₂ capture and pollution particle scrubbing separation. The utility emerges specially when there is a need of gas liquid contacting systems with heat and mass transfer applications. Due to the increased industrial demands of the superior and highly efficient columns researchers are working on the different structures and working column internals promoting gas liquid interface. Structured packing have most efficient and superior characteristics than the unstructured packings, nevertheless there are also disadvantages, particularly compared with the unstructured packing, but the design for these columns can be very effective in increasing the separation efficiency and decreasing the cost.

Supercritical fluid extraction (SFE) from liquid phase is usually carried out in packed extraction columns, with structured packing predominantly of the gauze type. The extraction of the natural raw materials to produce food ingredients, nutreaceuticals and phytopharmaceuticals or the fractionation of the beverages, citrous oils and lipids by using supercritical fluid technology is usually carried out in the packed extraction column with the structured packing. This type of packing performs very well, even under supercritical conditions, due to its relatively high surface area and void volume; these give rise to high mass-transfer efficiencies as well as high column capacities. Gauze structured packing has, nevertheless, some disadvantages with respect to unstructured packing. The main ones are its high cost and its low efficiency and capacity at high flowrates. An accurate column design is required to increase the separation efficiency and to decrease the associated costs.

Structured packing columns are widely used in chemical, biochemical, and petrochemical industries. It has been found that the flow pattern on different scales is of great importance in determining the process performance that using structured packing as their equipment internals.

The maximum column capacity is analysed by the pressure drop variation, the influence of the flow pattern in the packing, aerodynamics is required for design of the geometry of the corrugated sheets and get minimal pressure drop achieving high separation efficiency.

Propensity to structured packing's is driven by the minimal pressure drop per theoretical stage attained while achieving high separation efficiency, allowing reduction in energy dissipation, increasing loading capacity, and repelling flooding capacity to higher values.

This way we obtain a layered structure that is typical for structured packing, where we have alternating layers of sandwiches filled with catalyst pellets and empty sandwiches. In normal operation, the 'filled' channels will, due to capillary forces, provide pathways for the liquid to flow down. The empty channels will provide pathways for the vapour to go up at relatively low pressure drop. An interfacial area for gas-liquid mass transfer is provided by the metal gauze.

The high economic value represented by packed beds has driven an almost incredible number of studies investigating the chemical reactor engineering characteristics of packed beds, such as pressure drop, mass and heat transfer and dispersion, and continues to do so.

Detailed investigation of the fluid dynamic behaviour becomes essential for predicting the process performance and for developing more effective and optimal equipment internals. Liquid phase SFE has been carried out in extraction columns, with structured packing's particularly of the gauze type. In particular, it is necessary to determine the complex flow patterns of liquid and gas within the packing elements and to understand how they affect the pressure drop and mass-transfer efficiency. With the availability of such data is then possible to optimally design a column.

Computational fluid dynamics can be very helpful to characterize the flow inside the packed bed and evaluate the influence of the shape and geometry of the packing on the hydrodynamics and heat and mass transfer kinetics of the SFE packed column. New efficient geometries can be developed considering dry pressure drop by optimizing the geometric parameters. Also the wet pressure needs dry pressure drop for their calculations. One main and very important advantage of using CFD simulation is its potential to reduce the extent and number of experiments required to describe such a type of flow.

1.2 Types of packing

1.2.1 Different Representative Elementary units in structured packings

Representative elementary units (REU) were defined in many models as small structures reproducing the same packing element aerodynamics behaviour. Therefore, adapting these REU patterns in CFD simulations is more advantageous as they claim minimal computational

effort than one packing layer computational space. Different REUs and geometries of periodic elements used in the literature are summarized in Fig. 1.2.1.

The structured packing is tailored as a combination of four representative elementary units (REU), corresponding to the four main packing regions: entrance region, criss-crossing junction, two-layer transition, and channel-wall transition as shown in the Fig. 1.2.1(b). Another REU geometry was considered for the criss-crossing junction REU which consists of four channels, two are reversely positioned with the others given in the Fig. 1.2.1(a). The same criss-cross junction REU was adapted for another packing type in the Fig. 1.2.1(c). The periodic geometry corresponds to a box delimited by two corrugated sheets of which the width and height values corresponds.

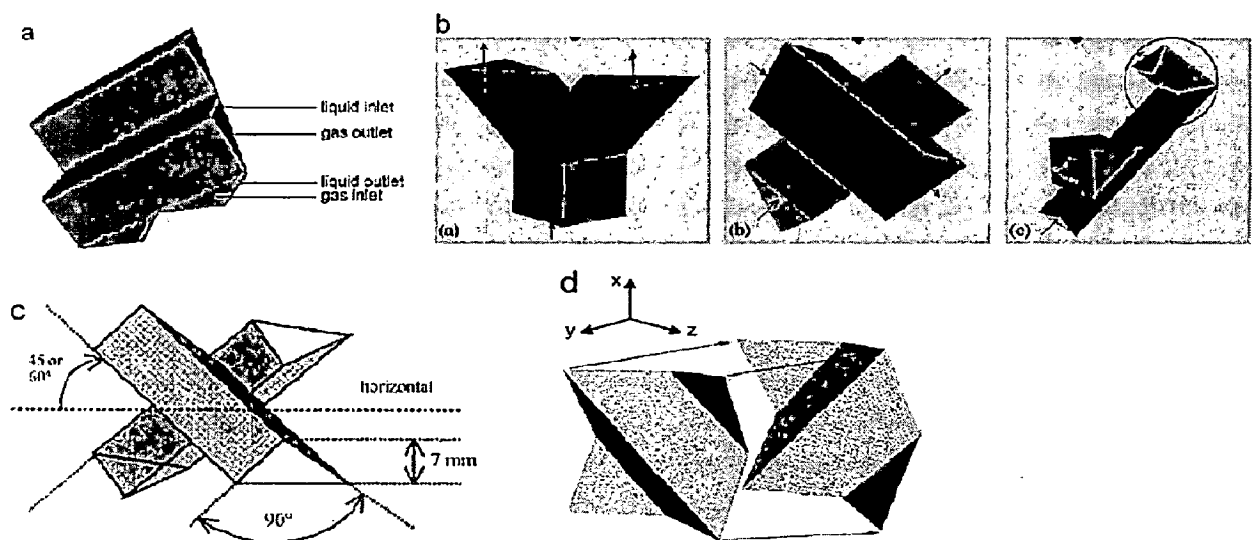


Fig.1.2.1 Different representative units from the literature: (a) Jiangbo REU (Jiangbo et al., 2009), (b) Larachi and Petre REUs (Larachi et al., 2003; Petre et al., 2003), (c) Raynal REU (Raynal et al., 2004) and (d) Raynal periodic element (Raynal and Royon-Lebeaud, 2007).

1.2.2 Different types of the commercial packings

There are different types of the structured packings are used in the industries of gas processing, chemical processing industry, process technology and equipment for oil refineries and crude oil production. They are shown as follows:

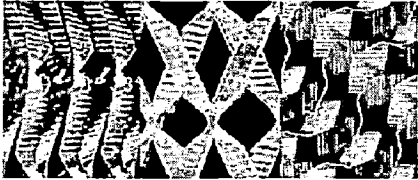
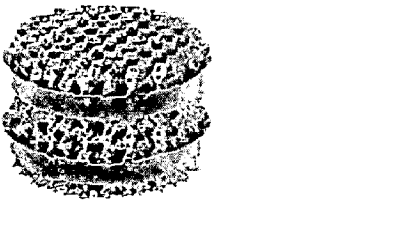


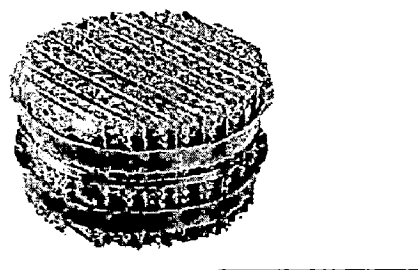
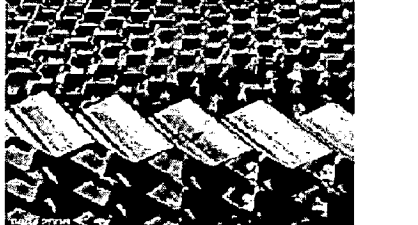
	<p>Rombopak, The unique open structure has been specifically developed for the distillation requirements of the fine chemical industry, pharmaceutical, Solvent recovery, Pilot plants and specially chemistry.</p>
	<p>Mellapak 250.Y/X A highly versatile packing type used in petrochemical industry in Quench columns, Refineries in Vacuum and atmospheric columns Absorption in natural gas drying.</p>
	<p>A new generation of structured packing Mellapak Plus is a capacity enhanced structured packing, it combines all advantages of the metal sheet packing Mellapak with new geometrical features.</p>
	<p>Sulzer metal gauze packing, It is used in the large number of the theoretical stages, where minimum pressure drop per theatrical stage is important, in the batch and continuous column, pilot columns and non-wetting liquids.</p>
	<p>Katapak-SP. This packing was developed to be applied in reactive distillation process; it has its application in synthesis of acetates, fatty acid esters, hydrolysis of methyl acetates.</p>
	<p>Mellagrid is used wherever the mechanical strength of the structured packing is concerned; its applications are in FCC main fractionators, wash section, atmospheric or vacuum tower.</p>

Fig 1.2.2 Different types of the commercial packings

1.3 Objectives

The objectives of the present work are as follows:

1. Selection of proper boundary conditions for the selected packing section as the whole column cannot be simulated.
2. Selection of turbulence model to predict dry pressure drop in the structured packings used in the packed towers.
3. Validation of simulated prediction from present work with the pressure drop results reported in the literature.
4. Hydrodynamics inside the structured packing.
5. Development of the new packing for the better performance in the packed column for the better mixing

CHAPTER 2

LITERATURE REVIEW

Prediction of pressure drop in distillation columns across the structured packing was subject to extensive studies. However, little work connecting the pressure drop with structured packing dimensions as geometric parameters, channel height, channel opening angle, and inclination angle was reported. Among the theoretical investigations on the flow behaviour in structured packing, *Hodso et al., (1997)* may be the first who used CFD method to simulate the flow pattern of the vapour phase on the micro-scale within the channels of the structured packing. On the laboratory scale experimental efforts were undertaken to relate empirical correlations to the a packing type used by adjusting the results equation results with the measured pressure drops values. (*Rocha et al., 1993; Billet andschultes, 1992*) but, the results are not valid for the extrapolation as they were dependant on the laboratory scale model (*olujic, 1999*). Moreover empirical models and experimental devices are unable to separate the contribution of the packing sheets or column walls and packing layers transition on the overall pressure drop because of the inexistence of such non-intrusive experimental approach.

Many theoretical approaches arise to overcome experimental limitations. One of the first mechanistic models aimed at studying the column diameter effect on the pressure drop, it shows that this diameter defines the number of the gas flow bends across the column walls, thus explaining the increasing pressure drop with decreasing column diameter (*Brunazzi and Paglianti, 1997*).

Stockfleth and Brunner (2001) studied the hydrodynamic behaviour, i.e., flooding, liquid holdup, and pressure drop of counter current columns with two random packings, Raschig rings and Berl saddles, and two gauze packing's, Sulzer CY and Sulzer EX, at temperatures between 313 and 373 K and pressure ranging from 8–30 MPa using carbon dioxide as the supercritical solvent and water and olive oil deodorizer distillate as liquid phases. They employed two models to correlate the experimental data: a sophisticated mechanistic approach based on the liquid holdup and a well known empirical approach for the flooding point. The experimental data for the dry pressure drop and the liquid holdup below the loading point are successfully correlated using modified models from normal pressure operation.

Another interesting model was published by *Oluji (1997)*, identifying the pressure drop

components, friction term and drag term. The friction term lies in the gas–gas friction at the interface at the crossing of gas flow channels, and the gas–liquid friction or gas packing friction in the absence of liquid flow. The drag component is the result of sharp change in gas direction near the wall zone and between rotated packing layers. Correlations were established for each friction component and for the drag term, with constants used to fit experimental results of the Montz-Pak B1 commercial packing type. Later, the author studied the influence of the column diameter on the total pressure loss (*Olujic, 1999*).

The assessment of the real efficiencies of these packing poses extreme difficulties related to the moderately high pressures involved in these processes. Computational fluid dynamics can be very helpful to characterize the flow inside the packing on the hydrodynamics. Important advantage of the CFD simulation is its potential to reduce the extent and number of the experiments required to describe such a type of flow. CFD commercial software is a powerful tool to predict hydrodynamics and fluids behaviour in many complex structures simplifying experimental devices and reducing related equipment costs.

A CFD approach was proposed to model the two phase flow in columns with structured packings (*Mahr and Mewes, 2007*). The authors considered that the gas flow undergoes an anisotropic resistance inside the packed bed, depending on the gas velocity magnitude and direction. To evaluate the pressure loss across the different direction angles with the columns axis, various sections with several packing sheet thickness were cut-out from the packed bed. The sections were fitted in a wind tunnel of rectangular cross section. The pressure drop over the sections was measured by blowing the air at various flow rates through the wind tunnel. The aerodynamics through these sections was also simulated using the commercial software Fluent. They showed a good agreement between measurements and the numerical results of the pressure loss, proving the effectiveness of CFD simulations. The minimal pressure loss values were obtained when the sections were cut-out in the direction of the packing channels.

CFD approach to predict the dry pressure drop in a structured packing column (*Larachi et al., 2003*) was made. The structured packing is considered to be as a combination of four representative elementary units (REU), corresponding to the four main packing regions: entrance region, criss-crossing junction, two-layer transition and channel-wall on which CFD simulations were performed.

On each REU, the RNG k- ϵ turbulence model is used to study the aerodynamics and calculated the individual pressure loss coefficient in each REU. The overall dry pressure drop is then reconstructed by summing accordingly the four contributions. This model was verified with the experimental overall pressure drop values from the literature.

To avoid the complex boundary condition on the open side of the packing channels in the previous model, another REU geometry was considered for the criss-crossing junction REU (*Jiangbo et al., 2009*). The new REU consists of four channels; two are reversely positioned with the others. The REU was studied with CFD simulations using the VOF method combined with the RNG k- ϵ model to study the hydro-aerodynamics and the mass transfer inside the REU. Based on *Petre and Larachi's* work, the same criss-cross junction REU was adapted for another packing type (*Raynal et al., 2004*). A detailed discussion of the influence of different mesh sizes and turbulent models (laminar, standard k- ϵ , RNG k- ϵ) on the pressure drop is presented.

A multiscale approach for the gas and liquid flow in a large size column: small scale, mesoscale, large scale (*Raynal and Royan-Lebeaud, 2007; Raynal et al., 2009*). At mesoscale the authors defined a new geometry and simulated the gas flow in the element. The periodic geometry corresponds to a box delimited by two corrugated sheets; the width and height values correspond, respectively, to the channel base and height dimensions. The packed sheets are modelled as solid walls with no-slip boundary conditions and periodic flow is considered on other open faces of the box. Simulations were applied using laminar and standard k- ϵ turbulence models. As simulations were performed with gas flow only, the liquid influence was taken indirectly from the two contributions correction of the gas velocity by including liquid hold-up value, and imposing a moving wall condition in a vertical downward direction. Simulated values of the friction term were compared with the overall experimental pressure drop results from the literature data, neglecting the drag term influence on the total pressure drop the laminar model provides better results than the standard k- ϵ model.

For simulating two-phase flow within a structured packed-bed, *Szulczewska et al. (2003)* built a two-dimensional model to calculate the gas-liquid interfacial area and study the mechanism of droplet formation and liquid film breaking during gas-liquid counter-current flow over the vertical flat and corrugated plate. Using the VOF approach, *Raynal et al. (2004)* successfully estimated the liquid film thickness and thus the liquid holdup in structured packing. *Haghshenas et al. (2007)* modelled a whole packing module and determined its pressure drop, these authors also studied the mass transfer inside structured packing by using a two sheet model in counter-current gas-liquid flow.

More recently *Mahr and Mewes (2008)*, proposed another approach to solve the problem of multiphase flow in structured packing. They started by computing the pressure drops for the structured packing along several different directions and transformed these pressure drops into a directional resistance factor, therefore they could specify the flow resistance everywhere

inside their computational model. They used this anisotropic flow resistance to simulate the whole packed column.

The commercial CFD software package, Fluent v6.3, was used to predict the velocity profiles and pressure drop inside the packing. Under turbulent flow conditions, realizable $k-\epsilon$ model was used which is the modification of the standard $k-\epsilon$ model with standard wall functions. The realizable $k-\epsilon$ model differs from the standard one in that it contains a new formulation for the turbulent viscosity and a new equation for the dissipation rate.

A CFD model is proposed to calculate dry pressure drop in structured packing of Sulzer type used in supercritical fluid extraction (*Fernandes et al., 2008*). Simulations were performed on two different computational domains: (1) box delimited by two packing sheets, (2) packing element module consisting of 13 porous sheets. Simulations were performed using laminar model and the realizable $k-\epsilon$ model. Simulations were carried out to determine the pressure drops of Sulzer EX at various gas mass flow rates and various conditions of pressure (0.1–30 MPa) and temperature (298–393 K) and good agreement was found between predicted and experimental pressure drops. The flow field inside the structured packing was also analyzed. The dry pressure drop obtained is a very important factor in the design of supercritical fluid extraction columns and is used in many correlations for the determination of wet pressure drop.

Fernandes et al. (2009) used computational fluid dynamics (CFD) to study the complex multiphase flow inside Sulzer EX structured gauze packing and to understand the influence of shape and geometry on the hydrodynamics of packed columns. He presented models for the estimation of both dry and wet pressure drops. A pseudo single-phase CFD model has been presented for the determination of wet pressure drops in the Sulzer EX structured gauze packing. Assumptions underlying the single-phase model were validated for the VOF model. They carried out Simulations to determine the dry and wet pressure drops of Sulzer EX packing for various gas and liquid mass flowrates and various conditions of pressure (8.0–26 MPa) and temperature (313–393 K). After comparing the numerical simulation and the experimental data available in the literature, good agreement was found.

Said et al. (2010) proposed a model to determine the dry pressure drop friction component. The gas was assumed to establish a fully developed turbulent flow inside the structured packing channels. The structured packing geometry consists of a combination of periodic elements. It was shown that the reproduction of one periodic element aerodynamics leads to determine the gas distribution and pressure drop inside the packed bed. Therefore, modelling the dry pressure drop through one periodic element is a meaningful representation of the dry

pressure drop over the packing. CFD simulations were carried out on periodic elements using different turbulence models: RNG k- ϵ , realizable k- ϵ , and SST k- ω . Simulations performed with the different turbulence models (RNG k- ϵ , realizable k- ϵ and SST k- ω) show that the SST k- ω model was the most suitable to predict the pressure drop and the aerodynamics behaviour of the structured packing. Thus a CFD model for the pressure loss friction component in the gas crossing triangular channels was developed.

The dry pressure drop proved to be an important design parameter, since it leads to the evaluation of the total wet pressure drop. Among the different dry pressure drop components, the friction term inside the corrugated sheet packing presents the major contribution to the pressure drop (*Petre et al., 2003*). Their study aims at calculating this friction term, by performing CFD simulations on geometric periodic elements representing the structure of the packing.

Hosseini et al., (2009) used computational fluid dynamics to study the hydrodynamic of structured packing's. The results showed that the k- ω was a suitable turbulence model for analyzing the flows in structured packings. A simple method was proposed for evaluating the liquid holdup based on the *Larachi (2001)* model, the calculated liquid film thickness in 2D framework, and the empirical correlation of *Brito et al., (1994)*. This method was used for estimating the wet pressure drop in 3D structured packing for loading region with good accuracy as well as computational economy. The process of liquid film formation was also discussed. It was shown that the two-phase flow computational model predicted the overall pressure drop of the bed reasonably well in the loading region, particularly well near the flooding regime. The process of liquid film formation on the packing surface was studied in details and the parameters that influence the liquid film thickness were discussed.

Luo et al., (2008) studied the channel opening angle is an important geometrical parameter of structured packing. In this work, the effect of channel opening angle on the performance of the column containing structured packing was investigated both numerically and experimentally. The simulation results showed that the pressure drop can decrease substantially and the liquid maldistribution can be effectively reduced when the channel opening angle decreases from 90° to 20° . In addition, a new modified structured packing was validated according to total reflux distillation experiment. It was shown that the pressure drop of the new packing could reduce by 35% and mass transfer efficiency could increase by 13% compared to the Mellapak packing having the same specific surface area. Based on the simulation results, decreasing channel opening angle can largely reduce useless pressure drop

stemming from the interaction of crossing gas streams, and lead to a better hydrodynamic performance.

Jiangbo et al., (2007) carried out the experiment work to serve the validation of the simulation in the Single-phase Flow in Structured packing. In this work he measured the velocity profiles of the single phase flow in the structure packing at the Reynolds numbers of 20.0, 55.7 and 520.1, using the Doppler velocimetry (LDV). Comparison shows that the flow pattern, velocity distribution and turbulent kinetic energy (for turbulent flow) on the horizontal plane predicted by CFD simulation are in good agreement with the LDV measured data.

Scala et al., (1999) centered their study on the hydrodynamics and energy transfer inside structured packing; for that purpose they produced a model incorporating three different types of flow: inside the valleys of the corrugations, flow crossing the valleys, and ideal mixture. The proposed geometry was rather simple and the calculations were made for four staggered packing elements.

Based on van Gulijk's work, *Higler et al., (1999)* and *van Baten et al., (2001,2002)* studied the liquid phase mixing and mass transfer within a catalytic packed bed reactor which contained Katapak-S structure. *Zhang et al., (2004)* proposed a CFD model to describe the liquid flow behaviour in a structured packing column without taking the gas-phase behaviour into account.

Using the VOF approach, *Raynal et al., (2004)* were able to successfully estimate the thickness of the liquid film and consequently the liquid holdup in a structured packing. Later, the same authors presented a multi-scale approach for CFD calculations of gas-liquid flow within large columns (2007). In their approach, the authors start by determining the thickness of the liquid film and holdup using a 2-D model. The gas velocity was then corrected using the estimated values of holdup and mean thickness of the liquid film, and the pressure drop in a periodic representative unit cell of the packing was calculated. Finally, from these calculations the authors obtain directional resistance coefficients, which allowed them to model the whole packed bed as a porous medium.

Khosravi et al., (2008) investigated turbulence model applications on two-phase flow simulation in a structured packing using CFD application. Dry pressure drop, irrigated pressure drop, mass transfer and heat transfer were studied by $k-\epsilon$, RNG $k-\epsilon$, $k-\omega$ and BSL turbulence models. By looking carefully in $k-\epsilon$ type models, these types of turbulence model could not predict flow characteristics inside complex geometries such as structured packing.

Baten and Krishna (2002) studied the gas phase mass transfer in the empty channels, and the

liquid phase mass transfer within the catalyst-packed channels, of the criss-crossing sandwich structures of KATAPAK-S using computational fluid dynamics. KATAPAK-S showed excellent radial dispersion characteristics, but due to the upheaval caused by the flow splitting at the crossovers, the mass transfer coefficient is significantly larger than that for fully developed flow in a single tube. The primary objective of his work was to extend earlier work to the study of liquid phase and gas phase mass transfer within the sandwich structures.

Valluri et al., (2005) presented the model describing the dynamic evolution of waves on laminar falling wavy film at low to moderate Reynolds numbers ($Re < 30$) over corrugated surfaces. This model was based on the integral balance method, which is used to simplify the analysis by assuming a parabolic velocity profile within the bulk of the film. The predictions of this model were compared to those obtained from a computational fluid dynamics (CFD) code for which no assumptions regarding the film velocity profile are made. The model predicts suppression of wave growth on a corrugated surface.

Gu et al., (2003) presented a two-phase flow CFD model using the volume of fluid (VOF) method for predicting the hydrodynamics of falling film flow on inclined plates, corresponding to the surface texture of structured packing. Using the proposed CFD model he investigated the influence of the solid surface microstructure, liquid properties and gas flow rate on the flow behaviour. From the simulated results it was shown that under the condition of no gas flow the liquid flow patterns are dependent on the microstructure of the plates, and proper micro structuring of the solid surface will improve the formation of a continuous liquid film.

Cerro et al., (1998) carried out a number of experimental and theoretical studies into liquid film flow on solid surfaces with macro and micro-texture structures. In their studies a film evolution equation with an approximation of the viscous long-wave for the Navier-Stokes equations was presented. However, the inertia term was neglected, which was important to determine the stability of a liquid film.

Soare et al., (2001) proposed a simplified mathematical model for liquid flow on corrugated metal sheets in which the effect of surface tension was included by assuming that the force generated is uniformly distributed over the entire flowing liquid film. Using analytical solutions the liquid film thickness, velocity profile, mean velocity and liquid flow rate was calculated. Using FLUENT software package, *Beata et al., (2003)* simulated two-phase counter-current flow in a plate-type structured packing. The effect of the liquid flow rates on the interfacial area formed on the surface of the structured packing was investigated, but the effective wetted areas estimated by the two dimension CFD model can be unreliable.

Petre et al., (2003), developed a combined mesoscale microscale predictive approach to apprehend the aerodynamic macroscale phenomena in structured packings. The proposed method consists in identifying recurrent mesoscale patterns (the representative elementary units, REU) wherein the constitutive microscale dissipation mechanisms occur. The dissipative phenomena that were identified to be important were: the elbow loss and jet splitting at the packed bed entrance, the elbow loss at the column wall, the elbow loss at the jump from one layer to another, and the collisional losses at the criss-crossing junctions. Each mechanism was simulated over a wide Reynolds number range spanning the pure creeping flow to the fully developed turbulent flow using three-dimensional computational fluid dynamics. Postulating addictiveness of dissipation, the overall pressure drop was reconstructed. The approach was validated using experimental dry pressure drop data for different packing types (Flexipac, Gempak, Mellapak, Sulzer BX and Montz-Pak).

The complexity of flow modelling is enhanced by the fact that the new generation of packed beds is designed as the multiscale structures (*van Hasselt et al., 1999*). Then, the application of the most detailed models is limited by their high computational cost. On the other hand, the mechanistic models are not sufficiently general. Thus, searching for the effective method of the specialised packing design, the concept of a hybrid method of flow modelling has been tested experimentally (*Tobis, 2000, 2001 and 2002*).

Ohujic et al., (2004) presented results of a large-scale experimental study to establish the relation between the quality of initial gas maldistribution, as created by common liquid collecting devices used in redistribution sections of packed columns, and the hydraulics of a structured packed bed. Additional, controlled gas maldistribution studies were conducted to observe the bed height needed to smooth out various types of initial misdistribution. Common low and high-pressure drop liquid collectors generated gas maldistribution of strikingly large extent, which was in order of magnitude or even larger than that associated with liquid distribution standards. From dry and wet experiments, it was appeared that the type of initial gas maldistribution influences the pressure drop of the bed.

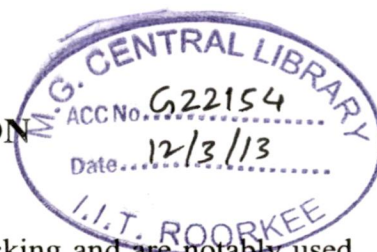
Tobis (2006) investigated the pressure drop and the fluid velocity profiles experimentally and numerically in the model packings of complex geometry. The numerical estimations were performed by means of the hybrid method involving the use of structural macro correlations. He demonstrated several examples of structural macro-correlations to predict the macro-scale flow behaviour in non-homogeneous packings. *Tobis (2008)* in his work combined experimental investigations and computational simulations into a hybrid method of complex phenomena modelling. In particular he applied thermo-anemometric technique and the multi-

scale methodology of modelling to investigate air turbulent flow within a rectangular container filled with spheres in cubic arrangement and different baffles alternatively inserted between the spheres. The model systems formed the complex geometric structures where three length scales were distinguished. Hence, the local fluctuations of air velocity were examined in the micro-scale determined by the size of the anemometric probe. The interstitial flow distributions, in turn, were investigated in the cell scale related to the sphere diameter. Thus pressure drop changes caused by the superficial flow distributions were analysed in the apparatus scale.

Beugre et al., (2010) performed numerical simulations of gas flow between two sheets of plastic Mellapak TM 250 Y using Lattice Boltzmann methods in laminar and turbulent regimes. Results were compared with experimental measurements and with known correlations. They were compared with simulations using a classical CFD code.

CHAPTER 3

MODELLING AND SIMULATION



The structured packing is more efficient than the unstructured packing and are notably used in many chemical processes involving separation, absorption, CO₂ capture and pollution particle scrubbing and supercritical fluid extraction. For the accurate column design it is necessary to understand the complex flow pattern of the gas or liquid within the packing and how they affect the pressure drop and hydrodynamics. Therefore in the present work different commercial structured packing are considered for studying the hydrodynamics by understanding the influence of the shape and geometry. Modelling and simulation are carried out with the different turbulence models to obtain the dry pressure drop. The different structured packing considered was Flexipac 1Y and Sulz EX. In section 3.1, 3.2 and 3.3 the description of different packing module with grid topology is discussed. The details of different turbulent models used are discussed in section 3.4.

The scope of the present work is to determine the effect of the geometric packing parameter variation on the dry pressure drop friction term inside the structured packing. The packing used for the CFD simulation for the dry pressure drop is Flexipac 1Y and the commercial packing SULZ EX. A periodic element consists of any volume cut out from the two packing sheet structure and whose duplication can produce the same geometry of the structured packing from which it is extracted. The structured packing chosen is the Flexipac 1Y commercial packing for two main reasons: (1) to check the representativeness of the bed aerodynamics characteristics by one periodic element for packing different, (2) because of its smaller dimensions, it enables a combination of a greater number of periodic elements, leading to a reasonable number of tetrahedral cells when meshing larger domains. CFD simulations are conducted on each periodic element with the use of commercial software package Fluent 6.3.26 combined with the geometric modelling and grid generation tool Gambit 2.4.6. The internal region of the packed bed, far from the column wall, can be reconstructed by connecting a network of then criss-crossing periodic elements.

3.1 Flexipac 1Y

3.1.1 Geometry description

A structured Flexipac 1Y packing type is defined by channel height, opening angle, and inclination angle. The details of the geometric parameters for the Flexipac 1Y are shown in the Table 3.1. The periodic element is modelled with the Gambit tool as a rectangular box with a proper dimension choice calculated from the channel dimensions. Geometry of periodic elements created by such a procedure is represented in Fig. 3.1(a).

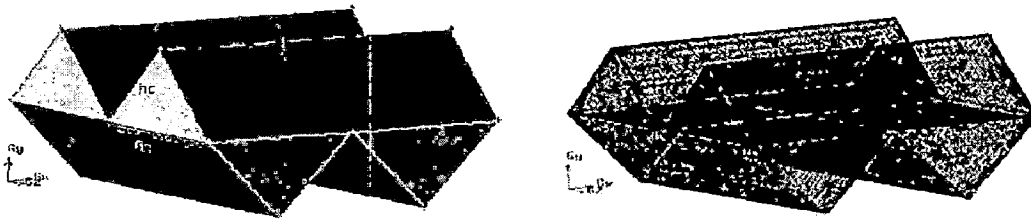


Fig. 3.1 (a) Channel direction slice for Flexipac 1Y (b) Grid topology for Flexipac 1Y

Table 3.1 Geometrical parameters for Flexipac 1Y packing used in simulations.

Packing type	a_g (m ⁻¹)	ϵ_g (%)	α_g (degree)	h_c (m)	b_c (m)
Flexipac 1Y	453	91	45	0.0064	0.0127

(Source: Said et al., 2011)

3.1.2 Grid formation and topology

A bottom-up strategy was used to generate the computational grid. First the vertices of the grid were defined, then the vertices were linked by lines, the lines generated surfaces and finally the surfaces originated volumes. The computational domain is meshed using the tetrahedral mesh grid with the size of 0.3 mm which is composed of 2,47,680 tetrahedral cells. On open faces of the periodic element, the flow is considered as periodic in both x- and z- directions. This is accomplished by combining each two periodic faces in one coupled face, and imposing periodic boundaries on each coupled face that are in the present case: top-bottom and left-right. The two sheets are modelled as solid wall surfaces with no-slip boundary conditions. Implementing the periodic conditions in Fluent 6.3 is possible by

specifying either the pressure gradient or the mass flow rate in a given direction. By imposing the pressure gradient in steady state mode across the z-direction, calculations continue until convergence when the mass flow rate becomes constant across the periodic faces. As the gas velocity profiles are similar on the two periodic faces, the periodic element is assumed to be extracted from a region where the gas flow is fully developed.

The dry pressure drop simulations are carried on the Flexipac 1Y for the different turbulence models. Simulations were conducted on the periodic representative element at different gas flow rates. The gas used in these simulations was air at ambient conditions $\rho_{\text{air}} = 1.225 \text{ kg/m}^3$ and $\mu_{\text{air}} = 17.894 \times 10^{-6} \text{ kg/m.s}$. The control volume domain considered is the periodic element in Fig 3.1(b).

The pressure velocity scheme used is simple and discretization used is second order upwind scheme for momentum, turbulent kinetic energy, specific dissipation rates. Simulations were carried out using the different viscous model, SST k- ω , RNG k- ϵ , realizable k- ϵ with standard wall functions and enhanced wall treatment and laminar flow for the low Reynolds number. The validations of simulated dry pressure drop values with that in the literature are discussed below.

3.2 SULZ EX packing

SULZ EX Packing is the commercial structured packing used in as a packed bed column for the chemical operations like extractions, absorption and various separations processes. In the present work two CFD models have been used to predict the dry pressure drop of a structured packing column at supercritical conditions. The two proposed geometrical models for the simulations consists of: (i) two contacting corrugated packing sheets (two packing sheet model) and (ii) ten contacting packing sheets. The first geometry mimics the volume existence between two packing sheets, and the second tries to mimic a whole packing element.

3.2.1 Geometry description

The geometry of the model corresponds to two packing sheets having the thickness of 0.31 mm included in a box is developed in the commercial software Gambit 2.4.6. The bottom up strategy is used in the construction of the geometry. The geometrical parameters of the packing are given in Table 3.2.

Table 3.2 Geometrical data of Sulz EX packing (*Source: Fernandes et al., 2008*)

Column internal diameter	24 mm
Packing	SULZER EX
Material	Gauze
Fractional void volume, ϵ	0.86
Specific surface area, a_s (m^2/m^3)	1710
Particle diameter, d_p (mm)	0.4912
Hydraulic diameter, d_h (mm)	1.886
Inclination angle, α (degrees)	45

Initially vertices are formed to develop the single face. The axis on the triangular face formed is rotated in the 45° inclination in the positive X and the triangular face is formed at this inclination axis at a given distance. Similarly for the bottom face the axis is rotated in the negative X axis for the upper sheet, faces are formed and volume thus gives the triangular channels which are criss-cross to each other. These volumes are copied in positive X directions and the computational domain for the two packing module is formed as shown in the Fig 3.2.

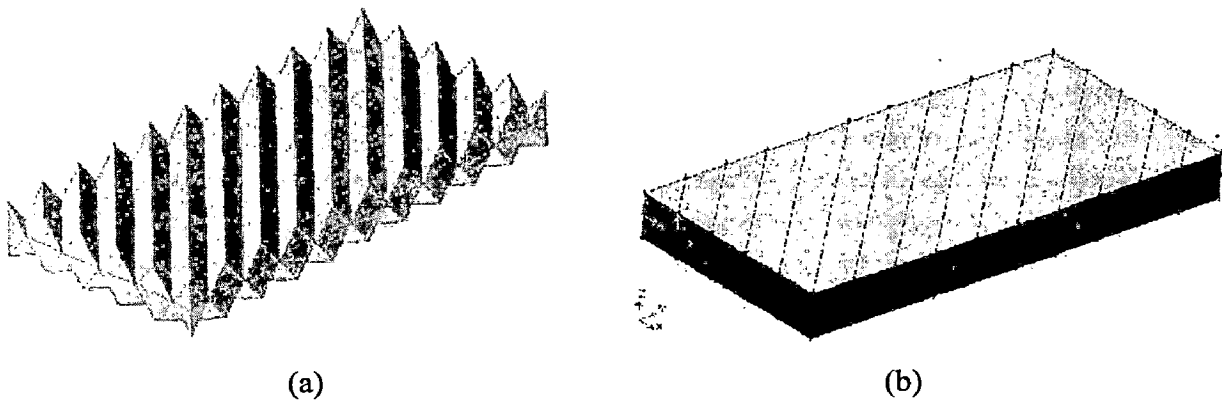


Fig. 3.2 (a) Two sheet packing structure with 45° inclination angle and (b) computational domain of two packing sheet included in a box.

3.2.2 Grid topology

The grid topology considered in the present work is similar to the mesh considered in the work of (Fernandes et al., 2008). The grid size considered was having the dimensions of 0.0003 mm. The inlet and the outlet faces are linked for the face meshes for defining it as periodic faces. The faces are meshed with Tri pave type scheme and volumes with the tetrahedral scheme. Thus computational domain is composed of 1,517,180 tetrahedral cells. The walls of the box in the x-direction are modelled as solid walls with non-slip boundary condition while the walls in the z-direction are modelled as translational periodic to account for the effect of neighbouring packing sheets. Periodicity of the flow was assumed to occur so the inlet and the outlet faces were defined as the periodic faces. Upper and the bottom planes are defined for symmetry, and the middle plane for the interior boundary conditions. The boundary conditions are reported in Table 3.3.

Table 3.2.1 Boundary conditions for the Sulz EX packing

Boundary	Boundary conditions
Wall +YZ & -YZ	symmetry
Wall +XY & -XY	walls
Wall +XZ & -XZ	periodic
Interior plane XY	interior
Translational Periodic walls	walls

The periodic conditions are possible by implementing either the pressure gradient or the mass flow rate in a given direction. By imposing the pressure gradient in steady state mode across the z-direction, calculations continue until convergence when the mass flow rate becomes constant across the periodic faces. The dry pressure drop is obtained at different mass flow rate value, which is the value calculated at the similar Reynolds no given in the literature. The pressure velocity scheme used is simple and discretization used is second order upwind scheme for momentum, turbulent kinetic energy and specific dissipation rates.

The simulations were carried out for CO₂ at supercritical conditions of 13.1 MPa at 313k with the viscosity of 6.24×10^{-5} (Data taken from the Stockfleth and Brunner for the two packing sheet models). Simulations were carried out using the different turbulence models, SST k- ω , RNG k- ϵ , realizable k- ϵ with standard wall functions and enhanced wall treatment and laminar flow for the low Reynolds number. The validations for the dry pressure drop values with that in the literature are discussed in Chapter 4.

3.3 SULZ EX packing Module

3.3.1 Geometry description

The second model or packing element module consists of ten sheets stacked together forming a packing element contained in a cylinder of diameter 0.024 m to mimic the interior. The module was surrounded by another cylinder with the diameter of 0.0288 m to mimic the wall. The distance from the interior to the wall is 0.0004 m. Due to the computational power constraints only one half of the actual packing element was modelled. But for the development of the flow the cylinder was extended in the positive Y and negative Y direction for the distance of 0.0024 m. For developing this model a bottom up strategy was used. The packing model developed for studying hydrodynamics is shown in Fig 3.3(a).

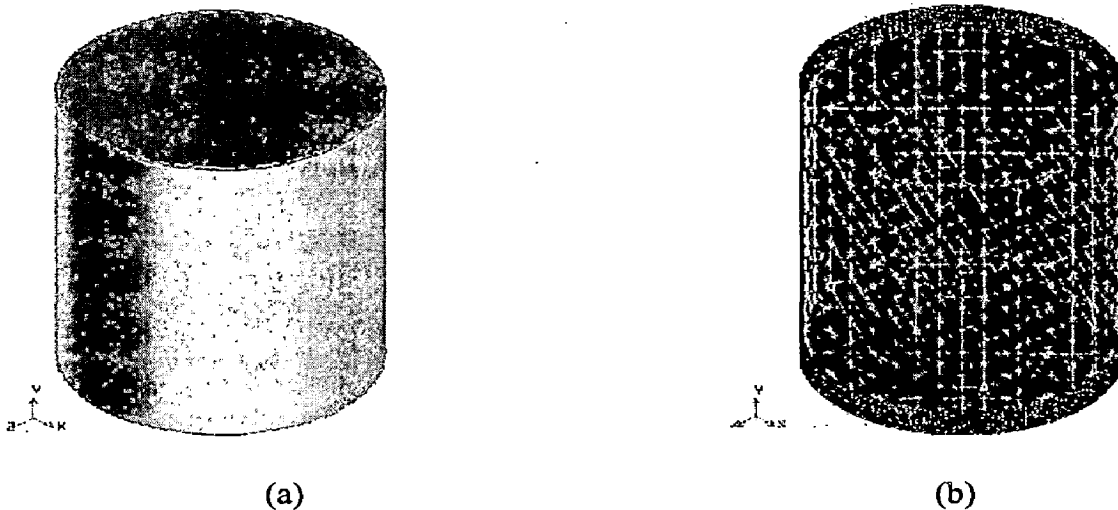


Fig. 3.3 (a) Computational domain and (b) grid topology of Sulz EX packing module.

3.3.2 Grid formation and Topology

The grid topology considered in the present work is shown in the Fig 3.3(b). The grid size considered was 0.00033 m as used by the Fernandes et al., (2008). The faces are meshed with Tri pave type scheme and volume with the tetrahedral scheme. Thus computational domain comprise of 2,49,4403 tetrahedral cells. The boundary condition at the column wall was defined as a interior, while the walls in the z-direction are modelled as translational periodic to account for the effect of neighbouring packing sheets. Periodicity of the flow in the axial direction, along the cylindrical tube was enforced by imposing periodic boundary conditions at the bottom and top cross-sectional planes of the computational domain. This is same as assuming that the flow is fully developed over the packing element. The plane between the

packing as given the interior boundary conditions. The boundary conditions for the packing model are reported in Table 3.3.1 while the outer cylindrical at a distance of 0.0004 mm from the inner cylinder is defined as wall with no slip boundary conditions, as given in the Table 3.3.1 The simulations were carried out for CO₂ for the similar supercritical conditions as that of the Sulz EX two packing sheet models.

Table 3.3.1 Boundary conditions for the Sulz EX packing module.

Boundary	Boundary conditions
Inlet & outlet wall	Periodic
Inlet & outlet	Interior
Interior planes	Interior
Inner cylinder wall	interior
Outer cylinder wall	wall
Translational Periodic walls	walls

3.4 Continuity and momentum equations

The discretization scheme for momentum used in simulations is second order upwind scheme and standard scheme for pressure. Pressure velocity coupling considered is simple with the 0.7 under relaxation factor for the momentum. The convergence criteria chosen is 10^{-5} for the continuity, turbulent kinetic energy (k) and specific dissipation rate(ϵ).

3.4.1 Turbulence models

3.4.1 a) k- ϵ turbulence models

The models of the Navier-Stokes equations are based on the transport equations of the turbulent kinetic energy 'k' and its dissipation rate ' ϵ '. One of the most prominent turbulence models, the k- ϵ (k-epsilon) model, has been implemented in most general purpose CFD codes and is considered the industry standard model. It has proven to be stable and numerically robust and has a well established regime of predictive capability. For general purpose simulations, the k- ϵ model offers a good compromise in terms of accuracy and robustness. For the three k- ϵ type models, the same equation is used for the turbulent kinetic energy equations in the RNG and standard k- ϵ models differ only in an additional term added in the RNG model, whereas this equation takes another form in the realizable k- ϵ model, based on the dynamic equation of the mean-square vorticity fluctuation and with respect to some physical constraints on normal stresses. Turbulent or Eddy kinetic viscosity is computed as a function of k and ϵ .

$$\mu_t = C_\mu \rho k / \varepsilon^2 \quad (1)$$

where μ_t is turbulent viscosity.

In the standard k- ε model, C_μ is a constant. The RNG k- ε model is an alternative to the standard k- ε model. In general it offers little improvement compared to the standard k- ε model. In the RNG k- ε model, C_μ is given by a differential equation to better handle low-Reynolds-number and near-wall flows. In the realizable k- ε model, C_μ is a function of the mean strain rate tensor and the mean rate of rotation tensor.

Compared to the standard model, the RNG k- ε is more accurate and reliable for a wider class of flows, as it is more responsive to effects of rapid strain and streamline curvature. The realizable k- ε model is more suitable for flows with strong adverse pressure gradients, separation or recirculation. It satisfies certain mathematical constraints on the Reynolds stresses which are consistent with the physics of turbulent flows.

Turbulence was modelled using the Realizable k- ε model, since it has been shown to give accurate results for flows involving rotation, boundary layers under strong adverse pressure gradients, separation and recirculation. In this model the transport equations for k (turbulence kinetic energy) and ε (turbulence kinetic energy dissipation rate) are

$$\frac{\partial(\rho k)}{\partial t} + \frac{\partial(\rho k u_j)}{\partial x_j} = \frac{\partial}{\partial x_j} \left[\left(\mu + \frac{\mu_T}{\sigma_k} \right) \frac{\partial k}{\partial x_j} \right] + G_k + G_b - \rho \varepsilon \quad (2)$$

$$\frac{\partial(\rho \varepsilon)}{\partial t} + \frac{\partial(\rho \varepsilon u_j)}{\partial x_j} = \frac{\partial}{\partial x_j} \left[\left(\mu + \frac{\mu_T}{\sigma_\varepsilon} \right) \frac{\partial \varepsilon}{\partial x_j} \right] + \rho C_1 S_\varepsilon - \rho C_2 \frac{\varepsilon^2}{k + \sqrt{\nu \varepsilon}} + C_{1\varepsilon} \frac{\varepsilon}{k} C_{3\varepsilon} G_b + S_\varepsilon \quad (3)$$

and the adjustable parameters are

$$\mu_T = \rho C_\mu \frac{k^2}{\varepsilon}$$

$$C_1 = \max \left[0.43, \frac{\eta}{\eta + 5} \right]$$

$$\eta = S \frac{k}{\varepsilon}$$

$$S = \sqrt{2 S_{ij} S_{ij}}$$

$$C_\mu = \frac{1}{4.04 + \sqrt{6} \cos \left((1/3) \arccos \left(\sqrt{6} \left((S_{ij} S_{jk} S_{ki}) / (\sqrt{S_{ij} S_{ij}}) \right) \right) \right)}$$

$$\frac{\partial k}{\partial t} + U_j \frac{\partial k}{\partial x_j} = P_k - \beta^* k \omega + \frac{\partial}{\partial x_j} \left[(v + \sigma_k v_T) \frac{\partial k}{\partial x_j} \right] \quad (5)$$

ii. Specific dissipation rate equation:

$$\frac{\partial \omega}{\partial t} + U_j \frac{\partial \omega}{\partial x_j} = \alpha S^2 - \beta \omega^2 + \frac{\partial}{\partial x_j} \left[(v + \sigma_\omega v_T) \frac{\partial \omega}{\partial x_j} \right] + (1 - F_1) \sigma_{\omega^2} \frac{1}{\omega} \frac{\partial k}{\partial x_i} \frac{\partial \omega}{\partial x_i} \quad (6)$$

3.5 Residence time analysis

The mixing inside the packed bed can be studied injecting a tracer at the inlet. The RTD calculations can be solved using the Species Transport Model equation. As a standard case for validation RTD analysis is carried out in a straight pipe having diameter as 0.01 m with 0.25m length for $Re = 100$ ($v = 0.01$ m/s). The boundary conditions given are wall at cylindrical face and velocity inlet for inlet and pressure outlet for the outlet. Initially the steady state flow field is solved in fluent. Then the tracer is injected in the domain. Solving the transient solution of the species equation the mean residence time can be calculated. The time calculated at outlet face where the concentration will be maximum $= 0.25/0.01 = 25$ sec which can be shown from the graph, which are the concentration obtained from the simulated results. Thus the retention time and the mixing phenomena inside the packing can be studied with the residence time distribution.

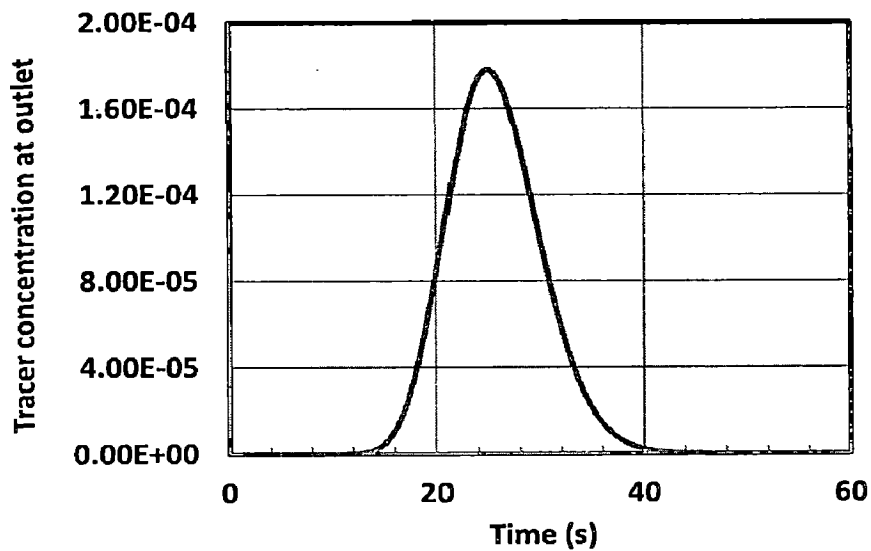


Fig. 3.5 Residence time distribution analysis

Table 4.1 Pressure drop predictions in Flexipac 1Y using different turbulence models.

V (m/s)	Re	F_s (m/s(kg/m ³))	$m \times 10^4$ (kg/s)	ΔP (Said et al., 2011)	Models	Simulated ΔP	Relative error (%)
1	577	1.225	2	58.53	Laminar SST k- ω Real k- ϵ (EWT) RNG k- ϵ Real k- ϵ (SWF)	52.58 62.1 53.28 98.74 98.92	10.88 6.1 8.96 68.69 68.14
1.5	865	1.8375	2.98	121.32	Laminar SST k- ω Real k- ϵ (EWT) RNG k- ϵ Real k- ϵ (SWF)	111.83 127.68 114.24 186.22 193.126	7.82 5.54 5.83 53.49 59.18
2	1153	2.45	3.97	206.04	SST k- ω Real k- ϵ (EWT) RNG k- ϵ Real k- ϵ (SWF)	225.86 189.67 293.94 317.415	9.61 7.94 42.66 54.65
2.5	1442	3.01	4.96	312.98	SST k- ω Real k- ϵ (EWT) RNG k- ϵ Real k- ϵ (SWF)	421.28 275 415.1 465.59	34.6 12.1 32.62 48.75
3	1730	3.675	5.96	442.15	SST k- ω Real k- ϵ (EWT) RNG k- ϵ Real k- ϵ (SWF)	658.52 375.95 556.53 646.53	48.93 14.97 25.86 46.22

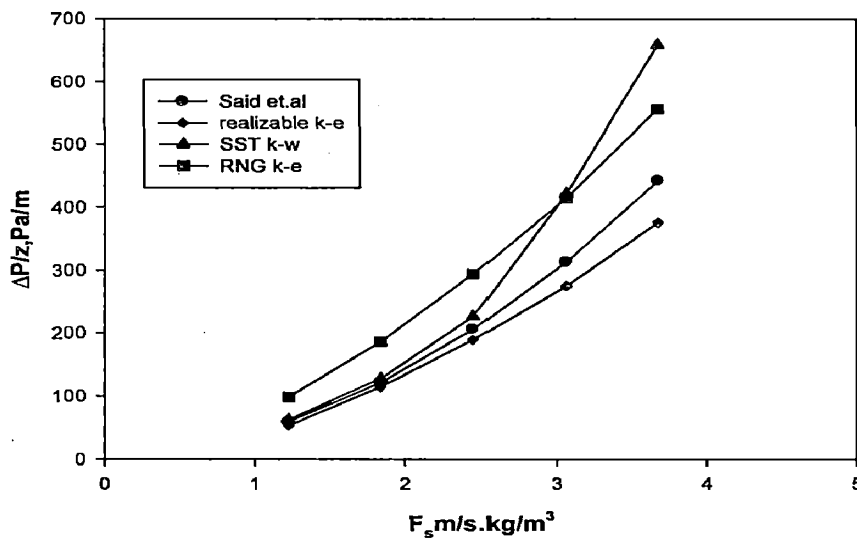


Fig. 4.1.1 Comparison of pressure drop in Flexipac 1Y for the different turbulence models.

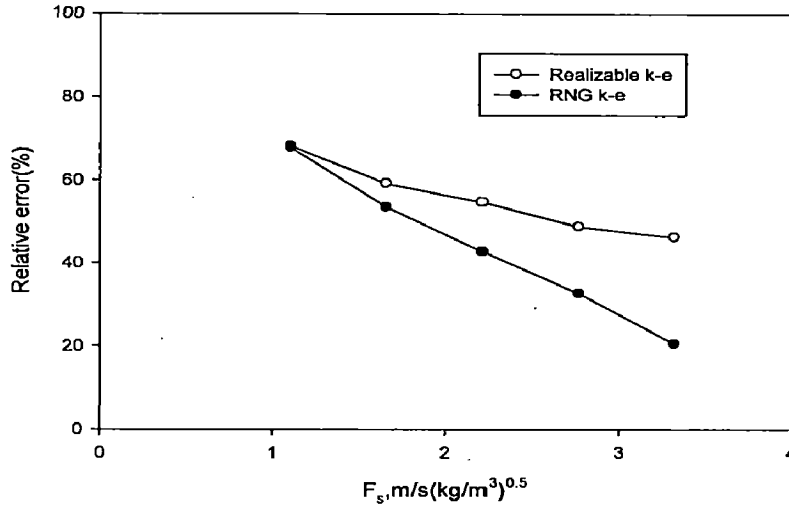


Fig. 4.1.2 Comparison of pressure drop values in Flexipac 1Y predicted by different turbulence models in terms of relative errors with the results of *Said et al. (2011)*.

4.2 Dry pressure drop in Sulz EX Packing

Another structured packing considered here for the hydrodynamics study and model validation is the Sulz EX commercial packing. The two sheet model is simulated for the different viscous models to calculate the dry pressure at the supercritical conditions of 13.1 MPa and 313 K with the viscosity of 6.24×10^{-5} kg/m.s for CO₂. The simulations were carried out for different mass flow rates (different Reynolds number) for which the experimental values are taken from the work of Stockfleth and Brunner (2001). The values for the resistance factor ψ and Re_G are taken from Stockfleth and Brunner (2001). The pressure drop per unit length ($\Delta P/H$) is calculated using the following relation:

$$\frac{\Delta P_0}{H} = \psi \frac{[(1-\varepsilon)\rho_G u_G^2]}{\varepsilon^3 d_p} \quad (7)$$

$$Re_e = \frac{\rho_G d_p u_G}{\mu_G} \quad (8)$$

where u_G is the superficial velocity of the fluid, ρ_G the fluid density, d_p the particle diameter and μ_G is the fluid viscosity. The simulations were carried by different viscous models as follows: Laminar, Realizable k-ε with pressure gradient effect and the SST k- ω . The cross sectional area at the inlet for the Sulz EX packing considered was 0.0001152 m².

The experimental values obtained from the Stockfleth and Brunner (2001) and simulated values for the different viscous models with their percent relative error are shown in the Table 4.2.1. It is observed that laminar model gives better results for the lower Reynolds number ranging from 200 to 400 and Realizable k- ϵ with pressure gradient effect for the higher Reynolds number. Relatively more deviation is shown by the SST k- ω model for the higher Reynolds number. The relative error shown by the SST k- ω is greater than 30% at low and higher Reynolds number. The percentage relative error can be seen from the Fig 4.2.1.

The resistance factor ψ values of the simulations are obtained using equation (1). The experimental and the simulated data for the resistance factors for different value at Reynolds number are reported in the Fig. 4.2.3. It is observed that the resistance factor values are comparable with the experimental values at low Reynolds number for laminar model and at higher Reynolds number for the realizable k- ϵ enhanced wall treatment with pressure gradient effect.

Table 4.2.1 Pressure drop prediction in Sulz EX packing two sheet model.

Sr no	Re	ΔP_{expt} Stockfleth and Brunner (2001)	$\Delta P_{k-\epsilon}$	Relative error (%)	ΔP_{lam}	Relative error (%)	$\Delta P_{\text{sst-kw}}$	Relative error (%)
1	214.4	1306.75	835.51	36.06	917.489	29.73	877.22	32.86
2	335.7	2707.8	1849.28	31.71	2405.14	11.17	2295.76	15.22
3	395.7	2977.68	2490.82	16.35	3517.02	18.11	3328.95	11.79
4	610.5	6212.9	5600.33	9.85	8274.289	33.17	8448.1	35.97
5	840	10839	10498.77	2.46	16241.36	49.84	16364.98	50.98
6	1038	16001.75	16070.75	0.43	24303.64	51.88	25224.85	57.63

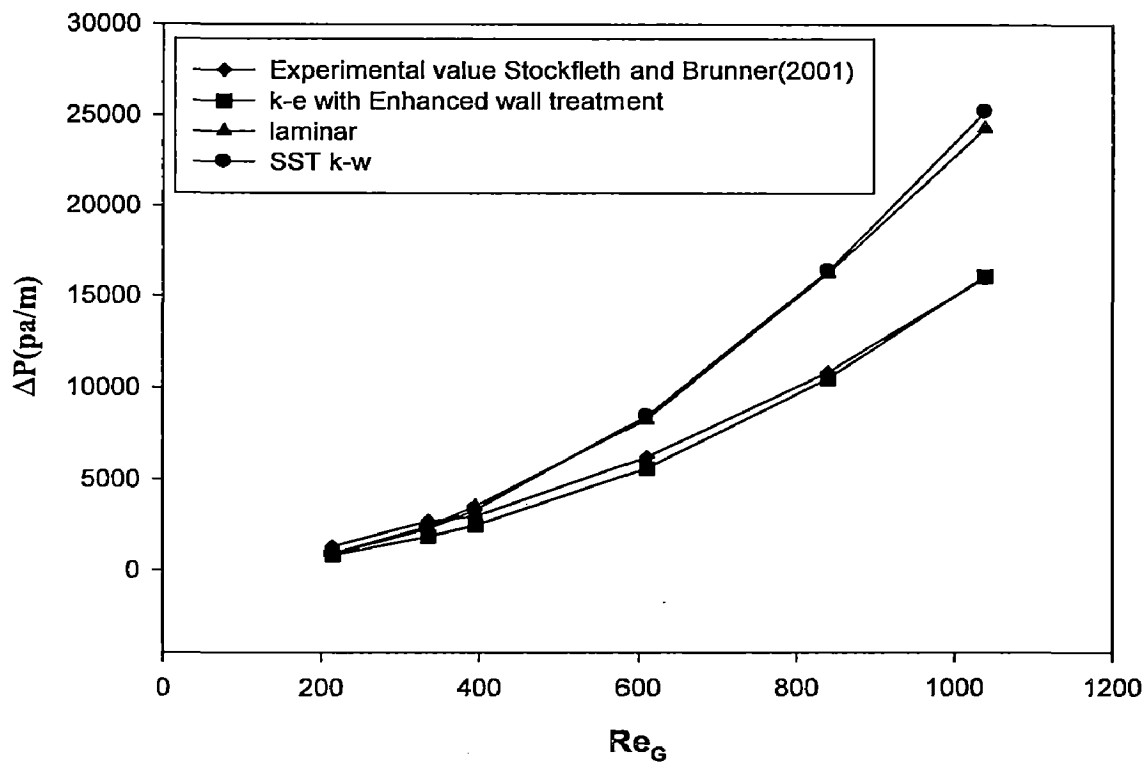


Fig. 4.2.1 Comparison of the pressure drop in Sulz EX packing for the different turbulence models.

Table 4.2.2 Resistance factor values with different viscous models for Sulz EX packing with two sheet model.

Sr. no	Re	ψ (Expt)	ψ (k-ε)	ψ (lam)
1	214.4	2.91	1.86	2.043
2	335.72	2.46	1.68	2.186
3	395.7	1.95	1.63	2.301
4	610.5	1.71	1.54	2.27
5	840	1.57	1.52	2.355
6	1038.1	1.52	1.53	2.33

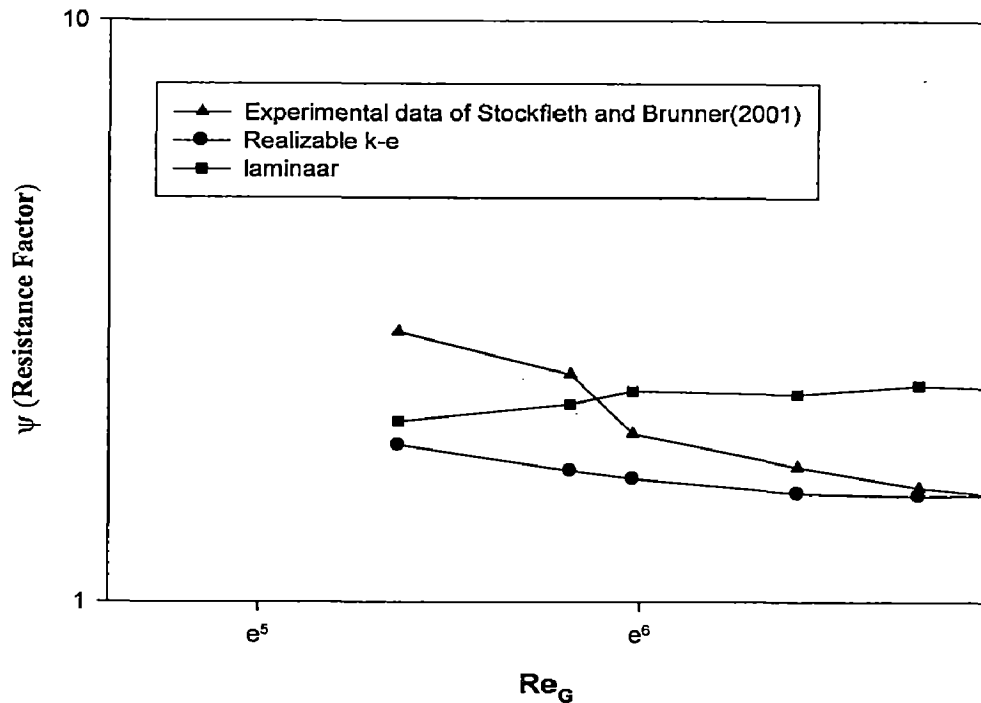
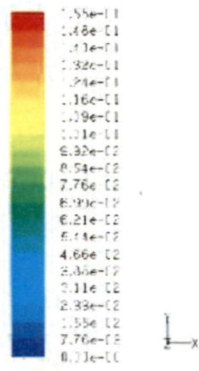
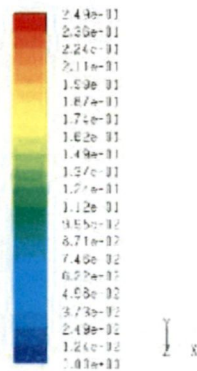
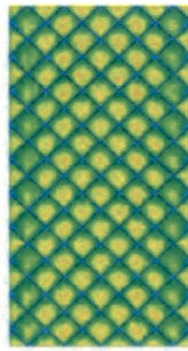


Fig. 4.2.3 Comparison for resistance factor between numerical simulation and the experimental data of *Stockfleth and Brunner (2001)*.

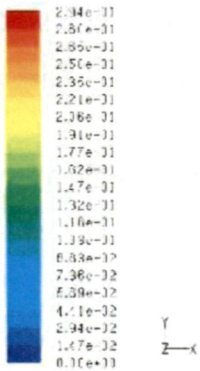
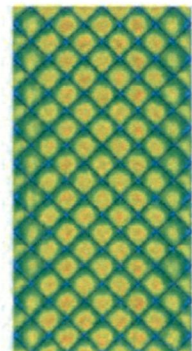
A plane between the two packing sheet is developed to analyse the flow pattern. The velocity contours at the above mentioned plane at different Reynolds number is given in Fig. 4.2.4. The contours on the entire interior surface shows that the flow is completely developed inside the packing. The interior plane is the plane between the two packing sheet. The contours of the velocity magnitude at the inlet and the outlet faces which are defined as periodic faces are shown in the Fig. 4.2.5. It is observed from Fig. 4.2.5 that the flow is developed in the inner triangular faces of the inlet. It is not developed for the upper faces due to the elongated orientation of the packing. Therefore due to the reduced cross-sectional area the pressure drop developed will be more in the Sulz EX packing. The contours developed on the plane which is defined at distance of 0.036 m from the inlet ensures that the flow is completely developed on the inner channel of the packing.



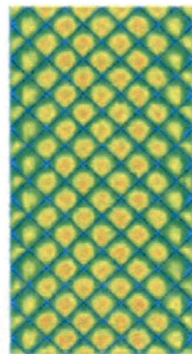
(a) Re =214



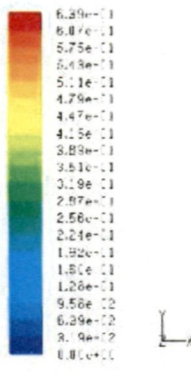
(b) Re =335



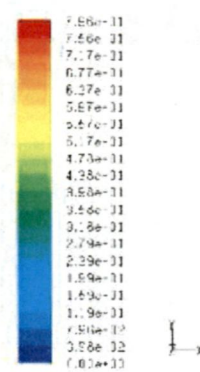
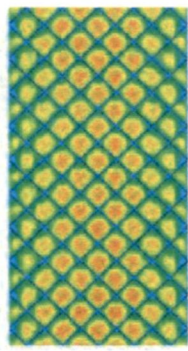
(c) Re =395



(d) Re =610



(e) Re =840



(f) Re =1038

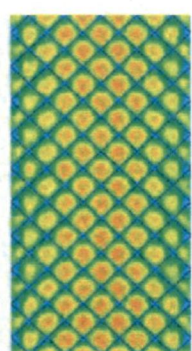
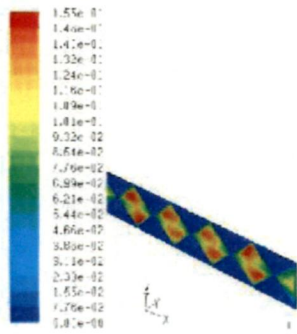
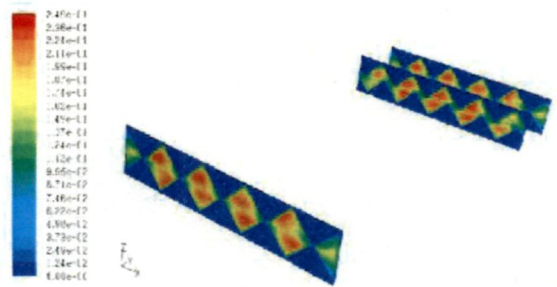


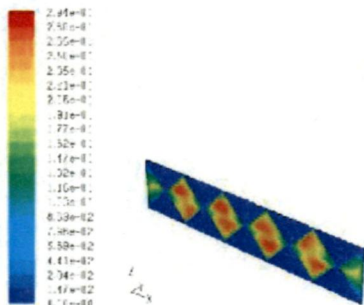
Fig 4.2.4 Velocity counters on the interior of the Sulz EX packing at different Reynolds number by using realizable k-ε model.



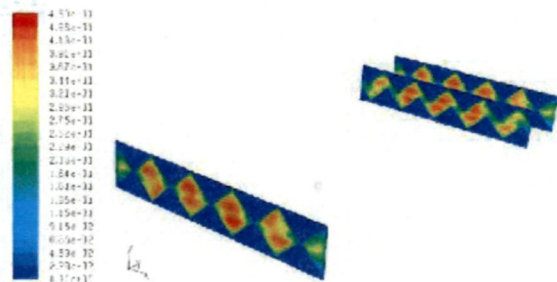
(a) Re = 214



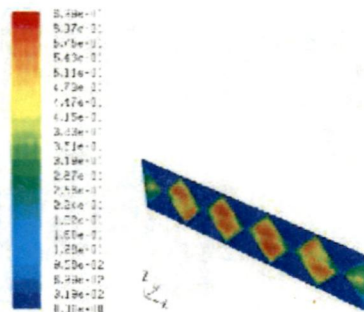
(b) Re = 335



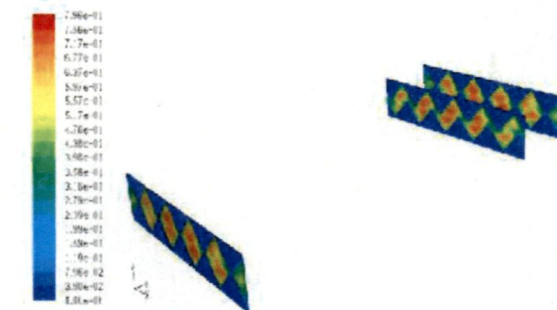
(c) Re = 395



(d) Re = 610



(e) Re = 840



(f) Re = 1038

Fig. 4.2.5 Velocity counters on the inlet, outlet and the middle plane of the Sulz packing at different Reynolds number by using realizable k-ε model.

4.3 Sulz EX packing Module

Simulation is carried out for the Sulz EX packing module for the realizable k- ϵ model with enhanced wall treatment and pressure gradient effects at the supercritical conditions of 13.1 MPa at 313k with the viscosity of 6.24×10^{-5} kg/m.s for CO₂. The cross sectional area at the inlet for the Sulz EX packing module considered was 0.000483 m². The periodic conditions in Fluent 6.3 by specifying the mass flow rate of 0.0515 kg/s in the Y direction is implemented. By imposing the mass flow rate in steady state mode across the Y direction, calculations continue until convergence when the mass flow rate becomes constant across the periodic faces. As the gas velocity profiles are similar on the two periodic faces, the gas flow is fully developed. The velocity counters for the velocity of magnitude 0.144 m/s on the periodic faces and the interior plane are shown in the Fig. 4.3(a). It is observed that the flow is completely developed on the various planes of the Sulz EX packing module as shown in Fig. 4.3(a).

To further understand the flow patterns inside the packing for the fully developed flow the particles of same physical properties inside the packing from the inlet faces were released and the pathlines were traced inside the Sulz EX packing module as shown in the Fig 4.3(b). It is observed from the Fig 4.3(b) that the flow has been formed on side walls of the Sulz EX packing, also the flow is continued after reversing the path from the wall, adding more shear stress and additional pressure drop. The increase in the thickness between the interior wall and the outer wall is recommended to study the hydrodynamics inside the packing module.

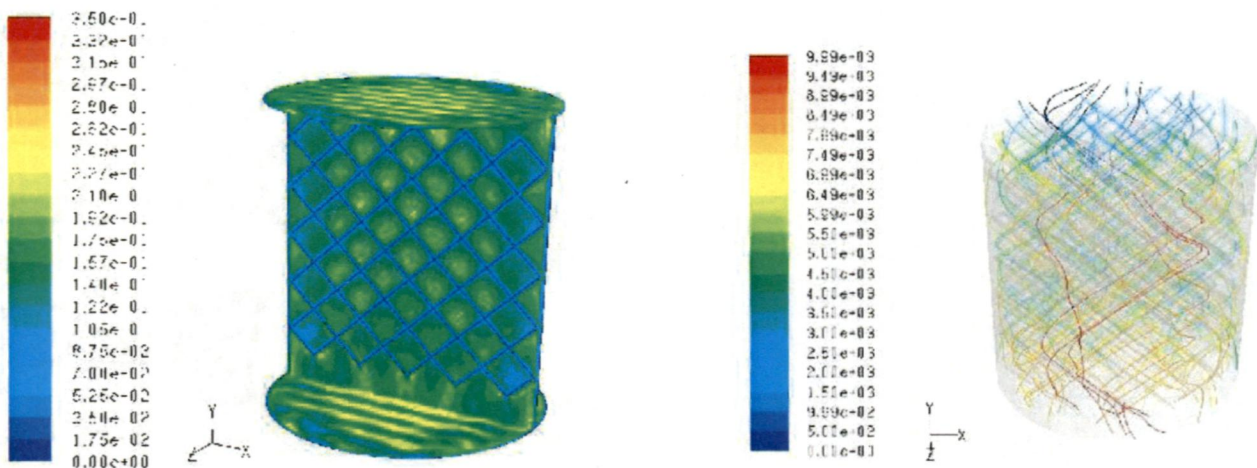


Fig. 4.3 (a) Velocity counters on the periodic and interior plane of Sulz EX packing module, and (b) pathlines inside the Sulz EX packing module

CHAPTER 5

CFD MODELLING OF ZIGZAG STRUCTURED PACKING

The maximum column capacity is defined by the pressure drop variation, which is one of the main variables of interest. A better understanding of the aerodynamics in structured packing is fundamental for design and investigation of new geometry of corrugated sheets for minimal pressure drop. A structured packing type is defined by their channel height, opening angle and inclination angle. Hydrodynamics inside the structure packing depends on these parameters. Pressure drop in columns equipped with structured packing is considered to involve two components: drag force due to the direction changes near the column walls and in the transition region between two packing layers rotated to each other by certain angle and friction force between the different gas flows inside the crossing triangular channels and with the packing solid walls.

Different types of commercial packing were studied such as Flexipac 1Y, Sulz EX and the effect of their changing geometry on the hydrodynamics and the pressure drop inside the packing. In the Sulz packing the two sheets has been rotated in the positive X and negative X direction in the structured pattern. This type of packing with uniform and complex computational domain inside the packing gives good mixing and larger surfaces internal area for the operations like supercritical fluid extraction using counter current process, gas absorption of CO₂ etc.

A new packing geometry is proposed in a zigzag pattern to increase the internal contact surface area and the mixing which will be more due to the directional changes of the flow from the walls in the packing due to the zigzag structure. The residence time in this type of packing will be more for the reactant and the efficiency of the column can be increased. We are interested in optimizing the pressure drop by comparing hydrodynamics with the structured available packing in the literature. The detail development and the modelling of the new geometry are given in next section.

5.1 Geometry description of Zigzag pack

The dimensions for the new geometry for the entire two packing sheet module included in the box are kept similar as for Sulz EX packing, only the orientation of the upper and the bottom packing is made in a zigzag pattern. In the Sulz packing the triangular domain of the sheet is

continuous and the flow is developed on the wall in the $-X$ and $+X$ direction, while in the zigzag packing the triangular sheet is not continuous, the sheet is alternately rotated in the $-X$ and $+X$ direction for the 45° of inclination for both upper and the lower sheet.

The geometry of the model corresponds to two packing sheets included in a box is made in the commercial software Gambit 2.4.6. The bottom up strategy is used in the construction of the zigzag geometry. The geometric data of the packing calculated are given as in Table 5.1

Table 5.1 Geometric parameter for Zigzag packing

Column internal diameter	24 mm
Packing	Zigzag Packing
Material	Gauze
Fractional void volume, ϵ	0.80
Specific surface area, a_s (m^2/m^3)	1611.12
Particle diameter, d_p (mm)	0.745
Hydraulic diameter, d_h (mm)	1.986
Inclination angle, α (degrees)	45

The characteristic diameter of the channels, d_p , and the hydraulic diameter d_h , are given by the relation.

$$d_p = 6(1 - \epsilon) / a_s \quad (9)$$

$$d_h = 4\epsilon / a_s \quad (10)$$

The thickness of the sheet used for the structured packing was 0.31 mm. Initially vertices are formed to develop the single triangular face and the axis made in the y direction on the base of the triangular face is rotated in the negative X direction for the distance of 0.0048 m and another triangular face is formed. Triangular domain is formed from the faces, further axis is rotated in the positive X direction and similar triangular volume which is rotated in the positive X direction is formed. Similarly the geometry is made for the bottom sheet in the reverse direction, volume thus gives the triangular channels which are crisscross to each other. The two sheet packing structure with the 45° inclination angle formed is shown in the Fig. 5.1. The computational domain considered for the simulation is the two packing sheet included in a box as shown in Fig. 5.1.

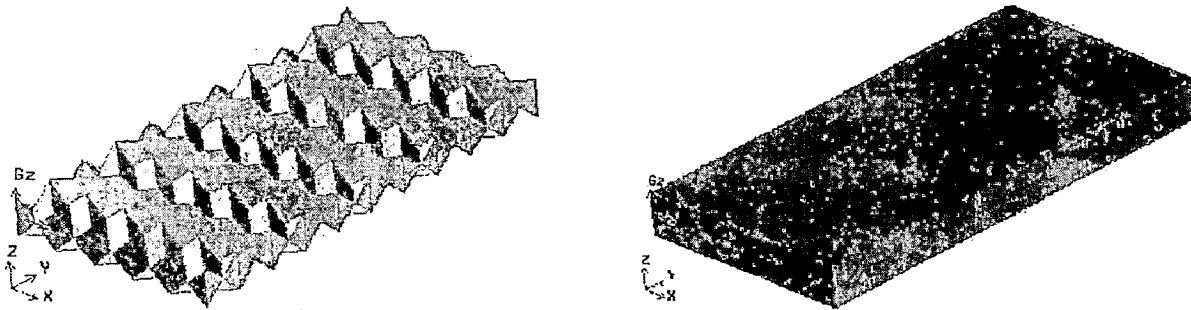


Fig. 5.1 (a) Two sheet Zigzag packing structure with the 45° inclination angle and (b) Computational domain of two sheets zigzag packing included in a box.

5.2 Grid topology

The structure is meshed with the same grid dimensions of 0.0003 m as taken for the Sulz EX packing and the inlet and outlet faces are linked for the face meshes for defining it as periodic in the Fluent. The grid topology for the zigzag packing is shown in the Fig. 5.2.1. The faces are meshed with tri pave type scheme and volumes with the tetrahedral scheme. Thus computational domain is composed of 1,501,972 tetrahedral cells which are approximately same with the Sulz EX packing. The walls of the box in the x-direction are modelled as solid walls with non-slip boundary condition while the walls in the z-direction are modelled as translational periodic to account for the effect of neighbouring packing sheets. Periodicity of the flow was assumed to occur so the inlet and outlet were defined as periodic faces. The packing sheet has the thickness of 0.31 mm. The boundary conditions are same as that defined for the Sulz EX packing.

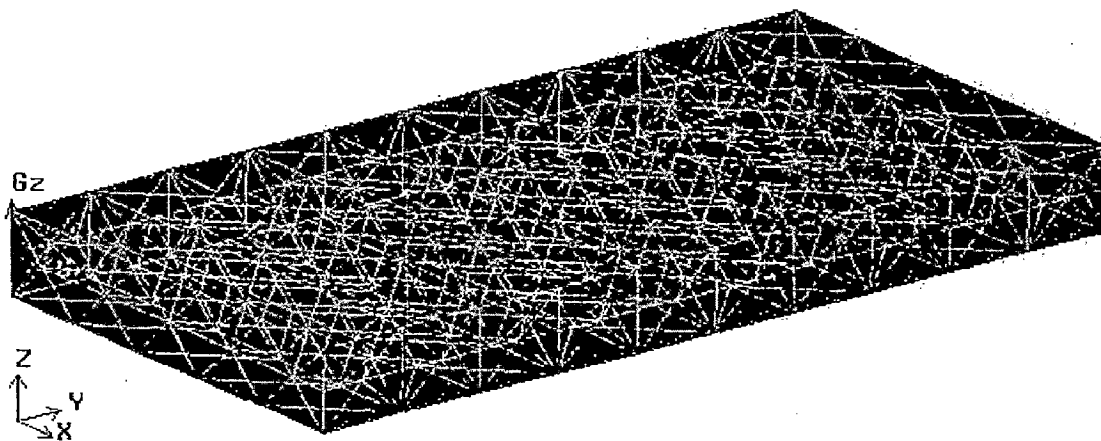


Fig. 5.2.1 Grid topology for the zigzag packing

Table 5.2 Boundary conditions for Zigzag packing

Boundary	Boundary conditions
Wall +YZ & -YZ	symmetry
Wall +XY & -XY	walls
Wall +XZ & -XZ	periodic
Interior plane XY	interior
Translational Periodic walls	walls

The periodic condition is implemented by specifying either the pressure gradient or the mass flow rate in a given direction. By imposing the pressure gradient in steady state mode across the z-direction, calculations continue until convergence when the mass flow rate becomes constant across the periodic faces. The dry pressure drop is obtained at different mass flow rate value, which is the value calculated from the given Reynolds number in the literature. The pressure velocity scheme used is simple and discretization used is second order upwind scheme for momentum, turbulent kinetic energy and specific dissipation rates.

The simulations were carried out for CO₂ at different supercritical conditions for data taken from the Stockfleth and Brunner (2001) for the two packing sheet models. Simulations are carried out using the different turbulence model, SST k- ω , Realizable k- ϵ with enhanced wall treatment and laminar flow for the low Reynolds number. Thus by obtaining the pressure drop for the new geometry, the hydrodynamics and the efficiency of the packing can be studied. The results obtained are discussed in the next section.

5.3 Hydrodynamics and pressure drop in the zigzag packing

The geometric parameters for the zigzag packing have been changed due to the change in the orientation of the two sheets with that of the Sulz EX packing. In the zigzag packing the total volume of the sheet used in the same computational domain is more as compared to the Sulz EX packing, therefore the specific surface area and void fraction will change respectively and for the given Reynolds number in the literature the velocity will vary due to the change in channel diameter. The zigzag pattern in the packing will vary the directional flow and add more collision for the fluid elements, due to the collision with the zigzag wall which will lead to the pressure drop variation. This pressure drop can be studied by simulating the computational domain with the different turbulence models.

The simulations are carried out by different viscous models (Laminar, Realizable k- ϵ with pressure gradient effect and the SST k- ω), for CO₂ flow at different supercritical conditions for different velocity and mass flowrates. The cross sectional area and the hydraulic diameter

of zigzag packing considered was 0.0001152 m^2 and 0.00198 m respectively. The Supercritical conditions considered are given in the Table 5.3.1. The simulated pressure drop for the different turbulence models at different supercritical conditions are given in Table 5.3.1.

Table 5.3.1 Experimental conditions and physical properties of the fluids used for pressure drop in the calculations in zigzag packing.

Dry pressure drops calculations for Supercritical CO ₂	Temperature (K)	Pressure (MPa)	Viscosity ($\times 10^5 \text{ Pa.s}$)	Density (kg.m^{-3})
	313	10.1	4.86	634
		12.6	6.07	730
		13.1	6.24	740

The pressure drop profile for the different turbulence models are shown in the Fig 5.3.1. It is observed that the pressure drop obtained for the Zigzag packing is greater in realizable k- ϵ model than laminar and SST k- ω , while in the Sulz EX packing pressure drop for the realizable k- ϵ model is less than laminar and SST k- ω . The increase in the pressure drop is linear approximately for all the models considered. When the zigzag packing is simulated at different supercritical conditions it is observed that the pressure drop is more for the higher supercritical pressure. From the Fig 5.3.3 it is observed that pressure drop in the Sulz packing is more than the zigzag packing at similar Reynolds number.

Table 5.3.2 Simulated pressure drop prediction for different turbulence models for the zigzag packing at 13.1 MPa.

Sr. no.	Re	u(m/s)	m(kg/s)	$\Delta P_{k-\epsilon}$	ΔP_{lam}	$\Delta P_{\text{sst-kw}}$
1	214.4	0.0243	0.002068	249.614	227.56	232.21
2	335.7	0.0383	0.00326	599.32	528.44	546.59
3	395.7	0.0448	0.00382	826.1	716.88	746.77
4	610.5	0.0691	0.00589	1924.25	1638.28	1739.85
5	840	0.0951	0.00811	3522.1	2997.4	3252.64
6	1038	0.1175	0.01	5429.7	4580.53	4917.72

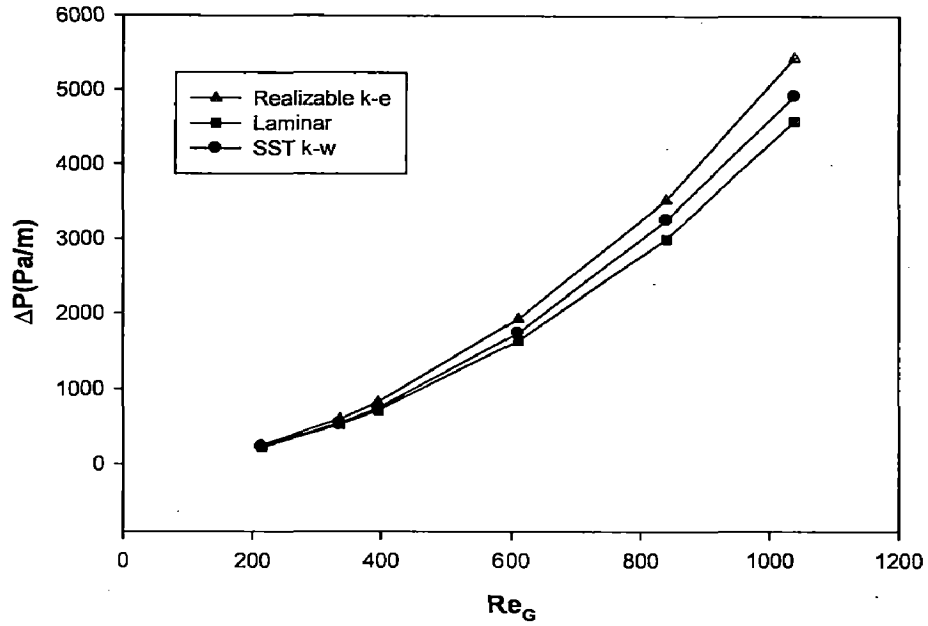


Fig. 5.3.1 Comparison of pressure drops of zigzag packing for different turbulence models.

Table 5.3.3 Simulated pressure drop in zigzag packing under different process conditions.

Sr. No	Re	10.1 MPa		12.6 MPa		13.6 MPa	
		u(m/s)	$\Delta P_{k-\epsilon}$	u(m/s)	$\Delta P_{k-\epsilon}$	u(m/s)	$\Delta P_{k-\epsilon}$
1	214.4	0.0239	175.76	0.022	236.81	0.0243	249.614
2	335.7	0.0374	416.86	0.03446	560.49	0.0383	599.32
3	395.7	0.0441	572.10	0.0406	772.28	0.0448	826.1
4	610.5	0.068	1332.00	0.0627	1793	0.0691	1924.25
5	840	0.0938	2482.42	0.0863	3349.32	0.0951	3522.1
6	1038	0.1159	3784.78	0.1067	5082.52	0.1175	5429.7

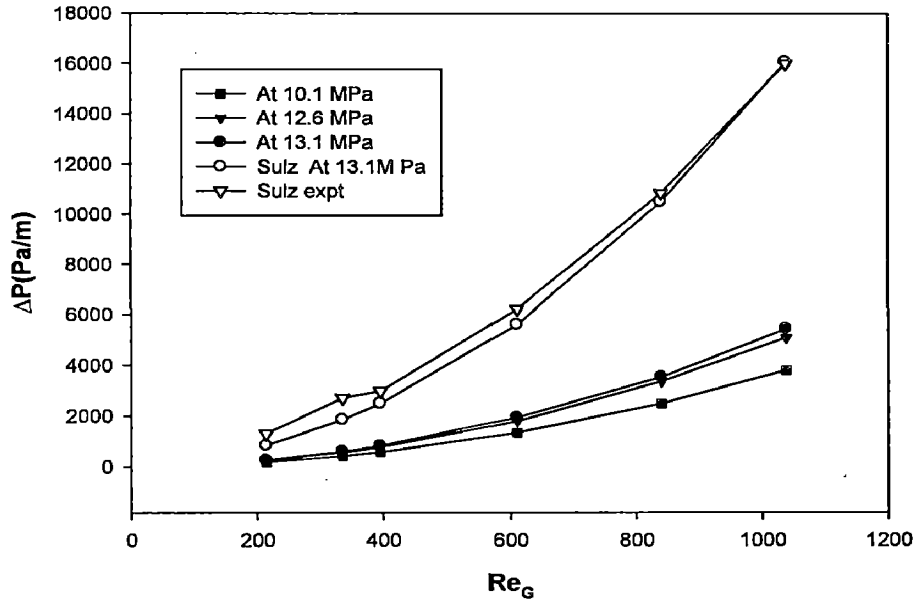


Fig. 5.3.2 Comparison of pressure drops of zigzag packing for the Realizable k-ε turbulence model at different supercritical conditions.

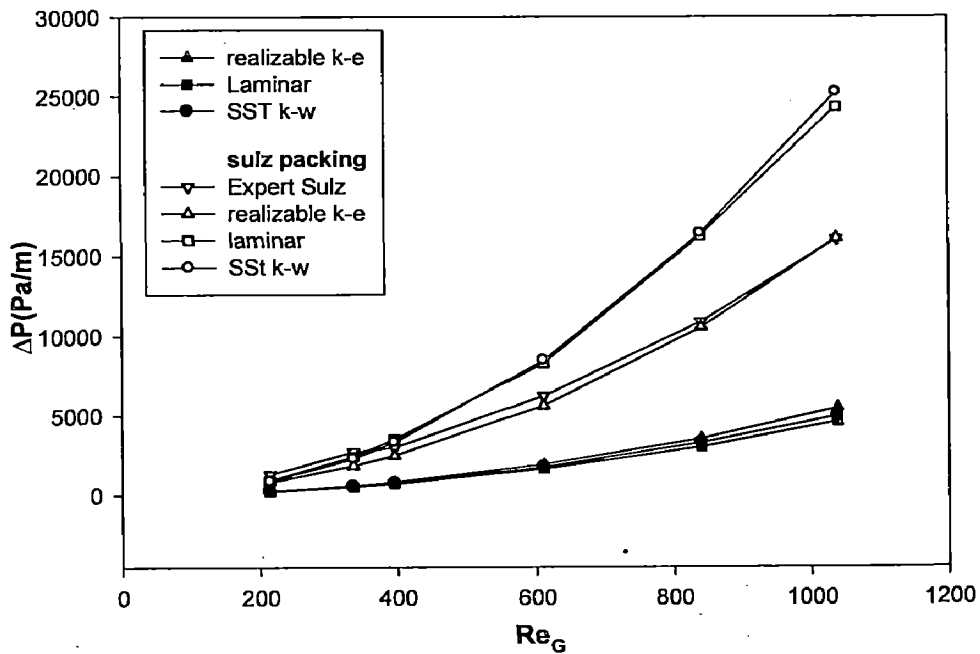
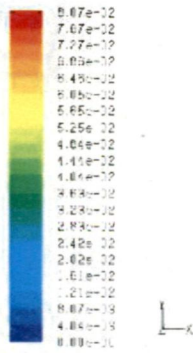
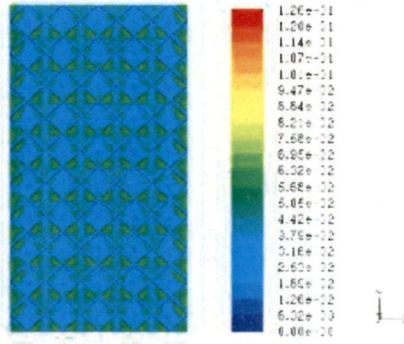


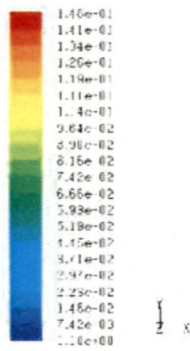
Fig. 5.3.3 Comparison of experimental and simulated values of Sulz EX packing with the simulated data for the zigzag packing.



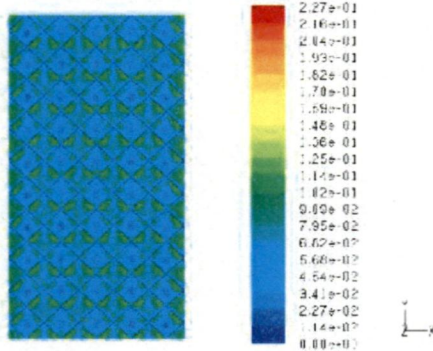
(a) $Re = 214$



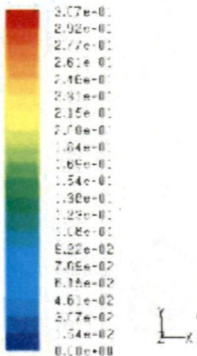
(b) $Re = 335$



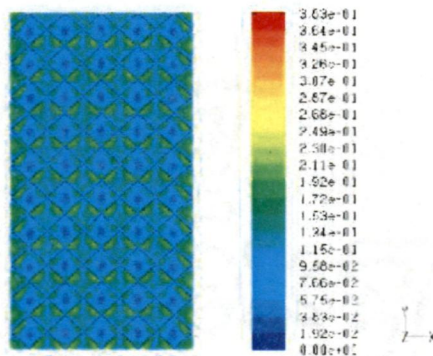
(c) $Re = 395$



(d) $Re = 610$

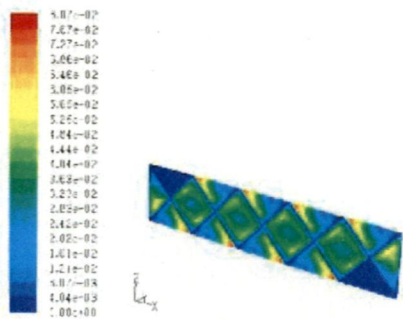


(e) $Re = 810$

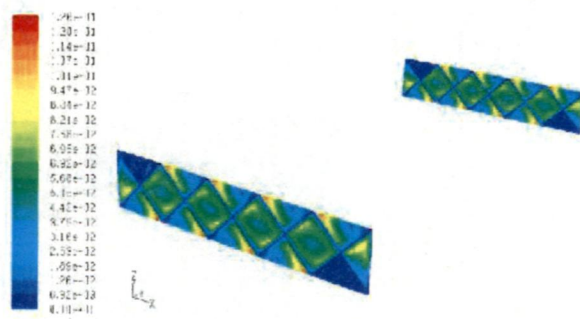


(f) $Re = 1038$

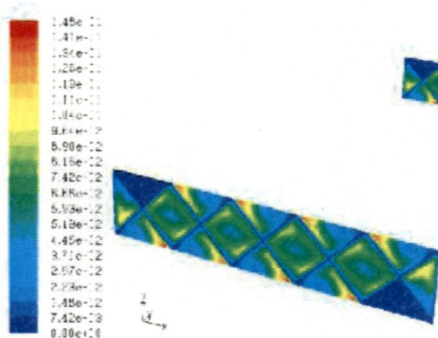
Fig. 5.3.4 Velocity counters on the interior of the zigzag packing at different Reynolds number by using realizable k- ϵ model.



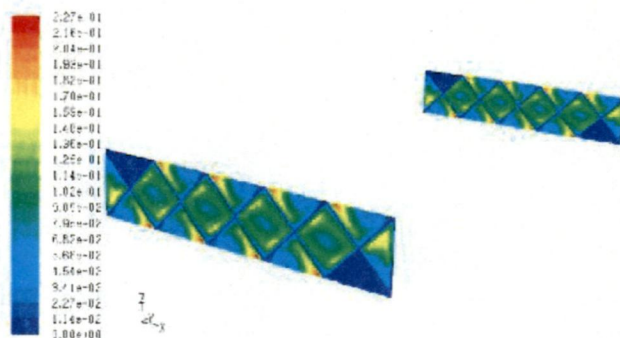
(a) Re =214



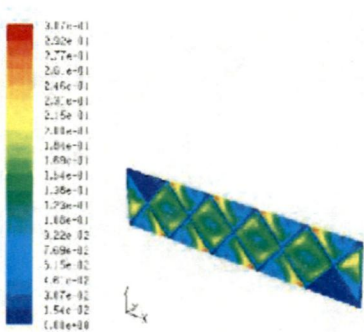
(b) Re =335



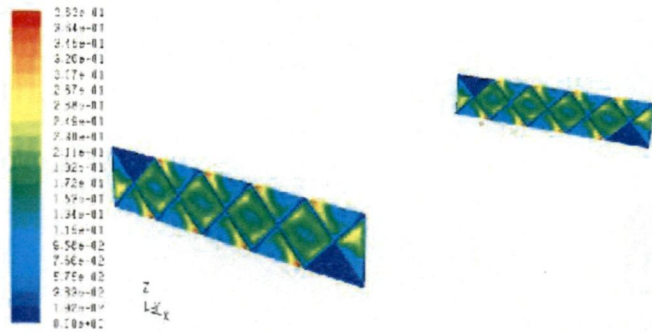
(c) Re =395



(d) Re =610



(e) Re =840



(f) Re =1038

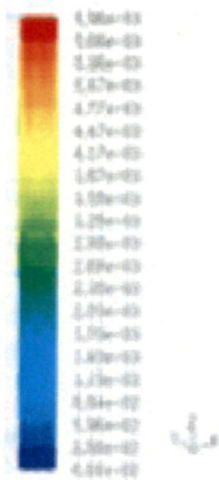
Fig. 5.3.5 Velocity counters on the inlet and outlet planes of the zigzag packing at different Reynolds number by using realizable $k-\epsilon$ model.

A plane between the two zigzag packing sheets is developed to characterize the flow pattern. The velocity contours developed on the above plane of the packing at different Reynolds number is shown above in the Fig 5.3.4. The velocity contours on the entire interior surface shows that the flow is completely developed inside the packing. The contours of the velocity magnitude at the inlet and the outlet faces which are defined as periodic faces are shown in Fig 5.3.5. The flow is developed on the entire inlet surface, on the inner and the outer triangular surface. The orientation of the zigzag packing sheet is in a zigzag pattern but in a straight direction, therefore for the complete inlet area the flow is developed. The orientation of the Sulz EX packing sheet is in the straight pattern but in the transverse direction therefore the flow is not developed in the outer triangular surface. Due to this parameter the pressure drop in the zigzag packing is less considerably the Sulz EX packing.

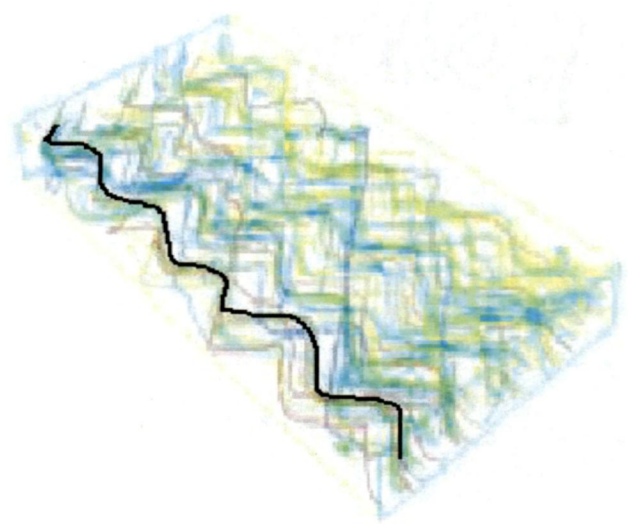
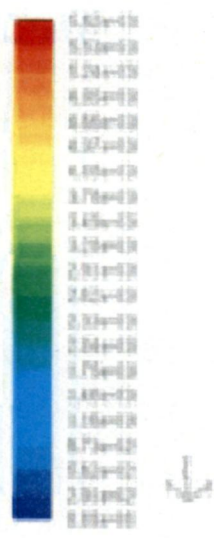
The simulations are performed for different supercritical conditions and at different turbulence models and it have been observed from the Figs 5.3.3 and 5.3.2 that the pressure drop in the zigzag packing is approximately three times less than Sulz EX packing. After considering the physical geometry of both the packing it is observed that, there could be more mixing in the zigzag packing as compared to the Sulz EX packing.

To understand the flow patterns inside the packing for the fully developed flow the particles of same physical properties inside the packing from the inlet faces were released and the pathlines traced inside the zigzag and Sulz EX packing are shown Fig 5.3.6(a). It is observed from the Fig 5.3.6(b) that the flow has been formed on side walls of the Sulz EX packing. Also the flow is continued after reversing the path from the wall, adding more shear stress and additional pressure drop.

The flow in the Sulz EX packing is showing irregular zigzag path in XY plane, leading to the increasing pressure drop. However flow in the zigzag packing is in the straight path, therefore no flow is developed on the side walls of the packing. It is following a uniform zigzag path in the YZ plane. Therefore it can be predicted that the path length travelled and the residence time of the particle in the Sulz EX packing is more as compared to the zigzag packing. Therefore the pressure drop in the zigzag packing is less as compared to the Sulz EX packing. The velocity vectors in the zigzag and Sulz EX packing at similar downstream length are shown in the Fig. 5.3.4(a) and Fig. 5.3.4(b).



(a)



(b)

Fig. 5.3.6 Pathlines inside the (a) Sulz EX packing and (b) zigzag packing.

CHAPTER 6

CONCLUSIONS AND RECOMMENDATIONS

6.1 Conclusions

In the present work the simulation were carried out on Flexipac 1Y packing and Sulz EX packing which is a structured packing, using commercial fluid dynamic software, FLUENT 6.3, ANSYS. The geometry was constructed using GAMBIT software, ANSYS. One of the objectives of present work to standardized the modelling approach to predict dry pressure drop in the structured packings used in the packed towers. Therefore different turbulence modelling approaches (laminar, standard k- ϵ turbulence model, realizable k- ϵ turbulence model with pressure gradient and SST k- ω turbulence model) were used to carry out pressure drop analysis in the Flexipac 1Y and Sulz EX. The simulated predictions from present work were validated with the pressure drop results reported in the literature. A new structured packing comprised of zigzag pattern is proposed based on the flow patterns in the existing structured packings. The hydrodynamic study in the proposed zigzag structure packing is carried out using CFD at similar conditions.

The simulations were carried out for Flexipac for Reynolds number ranging from 500 to 2000. The simulated pressure drop prediction with different turbulent models in the Flexipac structured packing is compared with the results reported in the literature. It has been observed that the relative error for pressure drop with that in the literature for the realizable k- ϵ model with enhanced wall treatment and pressure gradient effects is ($< 15\%$) and is ($> 30\%$) for the standard k- ϵ turbulence model, SST k- ω and the RNG k- ϵ . Similarly the simulations carried out for the structured Sulz-EX packing in the range of ($200 < Re < 1100$) as given in the literature. The relative error for pressure drop with that in the literature for the realizable k- ϵ model with enhanced wall treatment and pressure gradient effect is ($< 10\%$) for the Reynolds number (600–1000) and ($< 20\%$) for the Reynolds number (200–400).

From the literature results and the present simulated prediction for different turbulence models it has been observed that the Realizable k- ϵ model with pressure gradient effects is most efficient for hydrodynamic and pressure drop predictions in structured packings. It gives less relative error (less than or equal to 15%) as compared to other turbulence models. Results

obtained with Realizable $k-\epsilon$ model believed to be the most appropriate to use with the structured packing. F-factor was considered to represent the friction term of the pressure loss inside the structured packing. It has been found that as F-factor increases, the relative errors in the Realizable $k-\epsilon$ model and RNG $k-\omega$ model with respect to SST $k-\omega$ model decreases. The pressure loss friction component in the criss-crossing triangular channels in the Flexipac 1Y and inlet and outlet of the Sulz-EX packing is carried out. The proposed computational domain, a periodic element structure sliced from a packed bed and two sheet packing model established a fully developed gas flow inside channels.

The uniform pressure drop profile was developed for the zigzag packing by using the realizable $k-\epsilon$ model with the pressure gradient effects. The proposed computational domain, of the zigzag packing from a packed bed established a fully developed gas flow at the inlet and outlet inside channels. The pressure drop in the zigzag packing is found 3 times less than Sulz-EX packing due to the difference in the path travelled by the fluid inside the packing.

6.2 Recommendations

The CFD analysis inside the structured packing has given a good estimate about the hydrodynamics and the flow pattern inside the packing. The simulations carried on the Flexipac 1Y and sulz packing with the different turbulence models at different flow rate has given a good estimate for the usage of these models at different packing for the calculation of the pressure drop with the different parameters. It is proposed to use the similar efficient turbulence model will be used for the Sulz EX module for the future work in the CO_2 absorption process. Also the wet pressure drop inside the packing for CO_2 -capturing system will be analyzed to understand the hydrodynamics inside the column.

REFERENCES

- Beugre, D., Calvo, S., Crine, M., Toye D., Marchot P., 2011. Gas flow simulations in a structured packing by lattice Boltzmann method. *Chemical Engineering Science*, 66, 3742–3752.
- Brunazzi, E., Paglianti, A., 1997. Mechanistic pressure drop model for columns containing structured packings. *AIChE Journal*, 317–319.
- Brunner, G., 1998. Industrial process development in countercurrent multistage gas extraction (SFE) processes. *Supercritical Fluids*, 13, 283.
- Fernandes, J., Lisboa P.F., Simões, P.C., Mota, J.P.B., Saatdjian, E., 2009. Application of CFD in the study of supercritical fluid extraction with structured packing: Wet pressure drop calculations. *Journal of Supercritical Fluids*, 50, 61–68.
- Fernandes, J., Simões, P.C., Mota, J.P.B., Saatdjian, E., 2008. Application of CFD in the study of supercritical fluid extraction with structured packing: Dry pressure drop calculations. *Journal of Supercritical Fluids* 47, 17–24.
- Gao, D., Morley, N.B., Dhir, V., 2003. Numerical simulation of wavy falling film using VOF method. *J. Comp. Phys.* 192 (2), 624–642.
- Hirt, C.W., Nichols, B.D., 1981. Volume of fluid (VOF) method for the dynamics of free Boundaries. *Journal of Computatioanl Physics* 39, 201–225.
- Hodson, J.S., Fletcher J.R., Porter K.E., 1997. Fluid mechanical studies of structured distillation packings. *Institution of Chemical Engineers Symposium Series, AIChE, New York*, 142, 999–1007.
- Jiangbo, C., Chunjiang, L., Xigang, Y., Guocong, Y., 2009. CFD Simulation of Flow and Mass Transfer in Structured Packing Distillation Columns. *Chinese Journal of Chemical Engineering*, 17(3), 381-388.
- Jiangbo, C., Chunjiang, L., Yingke, L., Ying, H., Xigang, Y., Guocong, Y., 2007. Experimental Investigation of Single-phase Flow in Structured Packing by LDV. *Chinese Journal of Chemical Engineering*, 15(6), 821-827.
- Kumar, V., Aggarwal, M, Nigam, K.D.P., 2006. Mixing in the curved tubes. *Chemical Engineering Science*, 61, 5742-5753.
- Larachi, F., Petre, C.F., Iliuta, I., Grandjean, B., 2003. Tailoring the pressure drop of structured packings through CFD simulations. *Chemical Engineering and Processing*, 42, 535–541.

- Mahr, B., Mewes, D., 2007. CFD modelling and calculation of dynamic two-phase flow incolumns equipped with structured packing. *Trans IChemE, Part A*.
- Mahr, B., Mewes, D., 2007. Modelling of two-phase flow in structured packing. *Trans Ichem E* 85, 1112–1122.
- Nikou, M.R. K., Ehsani, M.R., 2008. Turbulence models application on CFD simulation of Hydrodynamics, heat and mass transfer in structured packing. *International Communications in Heat and Mass Transfer*, 1211–1219.
- Olujic, Z., 1997. Development of a complete simulation for predicting the hydraulic and separation performance of distillation columns equipped with structured packings. *Chemical and Biochemical Engineering*, 31–46.
- Olujic, Z., Behrens, M., Colli, L., Paglianti, A., 2004. Predicting the efficiency of corrugated sheet structured packings with large specific surface area”, *Chem. Biochem. Eng.* 18 (2), 89–96.
- Olujic, Z., Kamerbeek, A., De G.J., 1999. A corrugation geometry based model for efficiency of structured distillation packing. *Chemical Engineering and Processing*, 683–695.
- Petre, C. F., Larachi, F., Iliuta I., Grandjean B. P. A., 2003. Pressure drop through structured packings: Breakdown into the contributing mechanisms by CFD modelling. *Chemical Engineering Science* 58, 163 – 177.
- Raynal, L., Boyer, C., Ballaguet, J.P., 2004. Liquid holdup and pressure drop determination in structured packing with CFD simulations. *Canadian Journal of Chemical Engineering*, 82, 871–879.
- Raynal, L., Lebeaud, R, A., 2007. A multi-scale approach for CFD calculations of gas–liquid flow within large size column equipped with structured packing. *Chemical Engineering Science*, 62, 7196–7204.
- Raynal, L., Rayana, F.B., Royon-Lebeaud, A., 2009. Use of CFD for CO₂ absorbers optimum design: from local scale to large industrial scale. *Energy Procedia*, 917–924.
- Said, W., Nemer, M., Clodic, D., 2011. Modelling of dry pressure drop for fully developed gas flow in structured packing using CFD simulations. *Chemical Engineering Science*, 66, 2107–2117.
- Stockfleth, R., Brunner, G., 1999. Hydrodynamics of a packed counter current column for the gas extraction. *Industrial Engineering Chemistry Research*, 38, 4000–4006.
- Stockfleth, R., Brunner, G., 2001. Holdup pressure drop, and flooding in packed countercurrent columns for the gas extraction. *Industrial Engineering Chemistry Research*, 40, 347-356.

- Tobis, J., 2008. A hybrid method of turbulent flow modelling in packings of complex geometry. *Chemical Engineering Science*, 63, 2670–2681.
- Valluri, P., Omar, K., Matar, G.F., Hewitt, M.A.M., 2005. Thin film flow over structured packings at moderate Reynolds numbers. *Chemical Engineering Science*, 60, 1965–1975.
- Van Baten, J. M., Krishna, R., 2002. Gas and liquid phase mass transfer within KATAPAK structures studied using CFD simulations. *Chemical Engineering Science*, 57, 1531–1536.
- Van Baten, J.M., Ellenberger, J., Krishna,R., 2001. Radial and axial dispersion of the liquid phase within a Katapak-S structure: experiments vs. CFD simulations. *Chemical Engineering Science*, 56, 813–821.
- Yang, Z., Zhu, J., 1995. A new k- ϵ eddy viscosity model for high Reynolds number turbulent flows. *Comp. Fluids* 24 (3), 227–238.